

AD-A135 549

PASSIVE FILMS SURFACE STRUCTURE AND STRESS CORROSION
AND CREVICE CORROSION. (U) NATIONAL BUREAU OF STANDARDS
WASHINGTON DC J KRUGER ET AL. NOV 83 NBSIR-83-2790

1/1

UNCLASSIFIED

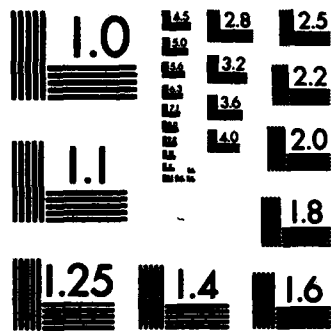
NAONR-18-69

F/G 11/6

NL

END

FORM
1-84
GPO



MICROCOPY RESOLUTION TEST CHART
NATIONAL BUREAU OF STANDARDS-1963-A

①

AD-A135 549

NBSIR 83-2790

**Passive Films, Surface Structure
and Stress Corrosion and Crevice
Corrosion Susceptibility**

**U.S. DEPARTMENT OF COMMERCE
National Bureau of Standards
Inorganic Materials Division
and
Metallurgy Division
Washington, D.C. 20234**

November 1983

DISTRIBUTION OF THIS DOCUMENT IS UNLIMITED

Final Report

**DTIC
ELECTE
DEC 8 1983
S H D**

**Prepared for
Office of Naval Research
Department of the Navy
Arlington, Va. 22217**

DTIC FILE COPY

88 - 12 08 080

NBSIR 83-2790

PASSIVE FILMS, SURFACE STRUCTURE AND STRESS CORROSION AND CREVICE CORROSION SUSCEPTIBILITY

J. Kruger, J. J. Ritter, G. G. Long, and M. Kuriyama

U.S. DEPARTMENT OF COMMERCE
National Bureau of Standards
Inorganic Materials Division
and
Metallurgy Division
Washington, DC 20234

November 1983

DISTRIBUTION OF THIS DOCUMENT IS UNLIMITED

Final Report

Prepared for

Office of Naval Research
Department of the Navy
Arlington, Va. 22217



Accession For	
NTIS GRA&I	<input checked="" type="checkbox"/>
DTIC TAB	<input type="checkbox"/>
Unannounced	<input type="checkbox"/>
Justification	<input type="checkbox"/>
By _____	
Distribution/	
Availability Codes	
Dist	Avail and/or Special
A-1	



U.S. DEPARTMENT OF COMMERCE, Malcolm Baldrige, Secretary
NATIONAL BUREAU OF STANDARDS, Ernest Ambler, Director

STRUCTURAL STUDIES OF PASSIVE FILMS USING SURFACE EXAFS

Jerome Kruger,¹ Gabrielle G. Long,¹ Masao Kuriyama,¹ and Alan I. Goldman²

¹Center for Materials Science, National Bureau of Standards,

Washington, DC 20234, (U.S.A.)

²Dept. of Physics, State Univ. of N.Y., Stony Brook, N.Y. 11794 (U.S.A.)

ABSTRACT

→ Iron K-absorption edge spectra were obtained from the passive films on iron for the dried films in air (ex situ) and for the films in the passivating solutions (in situ). The ex situ results demonstrate that, while the structures of the films are more disordered than the spinel-like iron oxides (e.g. α -Fe₂O₃), they are nevertheless closely related to these crystalline oxides. The in situ data shows evidence of a quite different structure, which may be due to the accommodation of hydrogen containing species into the structure. ←

INTRODUCTION

At the Fourth International Symposium on Passivity, Revesz and Kruger (ref. 1) pointed out that a vitreous structure provides a more effective passive film, and that the incorporation of "glass forming" elements, e.g., chromium, promotes the formation of such a desirable structure. This paper describes studies whose aim was to determine the structure of passive films on iron, and to explore the effect of chromium on the structure of these films using both near-edge and extended x-ray absorption fine structure (EXAFS).

Our earlier EXAFS studies (refs. 2 and 3), involving a specially designed system (ref. 4) to maximize surface sensitivity, were able to produce ex situ (but non-vacuum) EXAFS spectra of the passive films formed on iron in nitrite and chromate passivating solutions. Those studies found that the EXAFS signatures of the passive films resemble those of the spinel-like iron oxides, but that the chromate-formed film, which was found to contain chromium, may be more vitreous than the spinel-type oxides.

Our approach to the structural study of passive layers, as described in the present paper, aims to apply x-ray absorption spectroscopy to the in situ as well as ex situ investigation of the surface films on iron formed in two passivating solutions, one containing a glass forming element (a chromate solution), and the other not containing a glass

forming element (a nitrite solution). These studies extend our previous work in the following ways: 1. a synchrotron source with high resolution optics was used, enabling us to examine the absorption edge profiles; 2. thinner iron substrates were used, resulting in film spectra much less contaminated by the iron substrate signal; and 3. in situ spectra were obtained.

Two kinds of valuable information were extracted from the x-ray absorption spectra. First, the spectral features within ~ 30 eV of the iron K-absorption edge are sensitive to effects such as excitons and unoccupied final states of p-character. The positions in energy space of the K-edge of the thin films, relative to that for bulk iron, are directly related to the oxidation state, the coordination, and the degree of covalency in the bonding. These are important clues concerning the electronic structure of the films. The second kind of information derives from the fact that the extended x-ray absorption fine structure (from ~ 30 to 1000 eV above the absorption edge) is sensitive to the geometric structure in the vicinity of the absorbing atom. EXAFS spectra of model iron oxides have been taken to serve as empirical measures of the iron-oxygen and iron-iron phase shifts in these materials. Then, thin films on iron, formed in the inorganic passivating solutions, were measured, yielding structural parameters different from the model structures.

EXPERIMENT

The substrates used in these experiments were ~ 4 nm iron films deposited on glass slides in an ultra high vacuum system (base pressure $\sim 1 \times 10^{-8}$ torr). The iron films were immersed immediately after removal from the vacuum system into either 0.005 M potassium chromate or 0.1 M sodium nitrite. Passive films formed upon exposures of over one week to the passivating solutions have been shown (refs. 5 and 6) to have structure, composition and formation kinetics similar to those passive layers that form in Fe^{++} - free solutions by anodic oxidation.

After immersion in the passivating solutions for more than a week, the slides were removed, rinsed in distilled water and spectroscopic grade ethanol, and dried in a stream of pure nitrogen. Near-edge and EXAFS measurements were carried out on the passivated specimens either in air (ex situ) or in a specially constructed cell (ref.4) for in situ measurements. The spectra were taken at the C-1 station at the Cornell High Energy Synchrotron Source (CHESS). This station has a double flat crystal Si(111) monochromator with fixed exit position, suitable for this experiment. Data were taken in the

fluorescence mode using MnO_2 filters in front of the detectors to reduce the signal due to scattering. An array of three detectors was used to accumulate data simultaneously during each scan. Data near the edges were taken in 0.5 eV steps, while EXAFS data was taken in 3 eV steps. Data collection time for each set required more than one CHESS fill (2-4 hours of running time), and duplicate sets were acquired for each in situ and ex situ case.

RESULTS

The edge structures we measured are shown in Figs. 1 (ex situ and in situ nitrite-formed films) and 2 (ex situ and in situ chromate-formed films). The shapes of the in-situ and ex-situ film profiles are very different from each other. One can examine how different they are by taking the slope and plotting the derivative spectra. Fig. 3 shows the derivative spectra of the profiles in Fig. 1, and Fig. 4 shows those for the profiles in Fig. 2. It is rather striking that the edges from the two ex situ samples resemble one another much more closely than they resemble their respective in situ spectra. Furthermore, the ex situ edge results are also very similar to our edge data for $\gamma-Fe_2O_3$, indicating again a close relationship between these structures. For the in situ derivative results, we see two peaks for the chromate-formed film and one peak and a diminished second peak for the nitrite-formed film. While these two results resemble one another more closely than they do the respective ex situ data, there remain differences between them. Further analyses of this data will be forthcoming in a future publication (ref. 7).

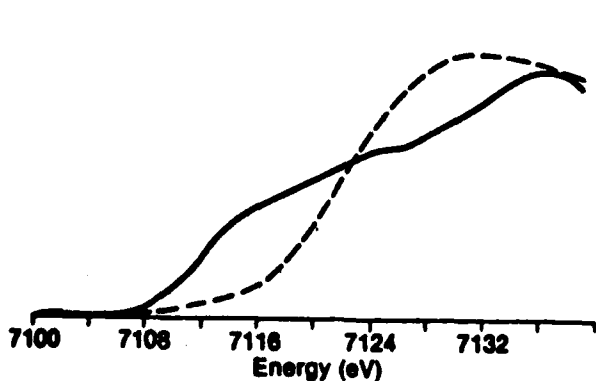


Fig. 1. K-edge profiles versus energy for the nitrite-passivated ex situ (--) and in situ (—) films.

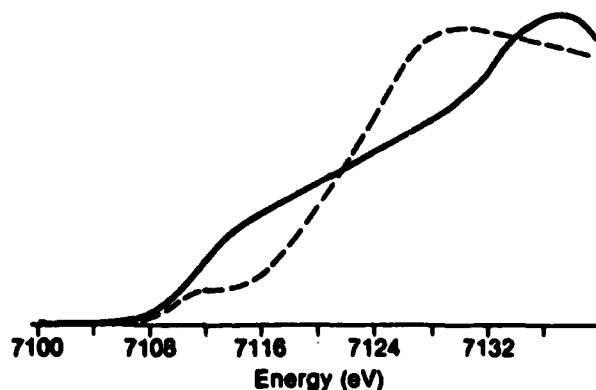


Fig. 2. K-edge profiles versus energy for the chromate-passivated ex situ (--) and in situ (—) films.

The magnitudes of the Fourier transforms of the in situ and ex situ nitrite data and chromate data are shown in Figs. 5(a) and (b). As was shown earlier (refs. 2 and 3) the ex situ results for the passive films formed in the two different passivating solutions are quite similar. Since there is less bulk iron signal here than in refs. 2 and 3, the resemblance between these passive film results and the data for the crystalline $\gamma\text{-Fe}_2\text{O}_3$ is much stronger. Both films appear to be more disordered than the model $\gamma\text{-Fe}_2\text{O}_3$, with the chromate-formed film showing the less order of the two. The in situ results, shown in Fig. 5(b), suggest that these structures, again while related to each other, are different from the ex situ structures. Also, it appears that the in situ structures differ from one another more than the ex situ structures do. All of this is consistent with the observed changes in the Fe K-absorption edges and the derivative spectra shown in Figs. 1-4. The details of the analysis will be presented elsewhere (ref. 7) since the present purpose is to give an overview of these results.

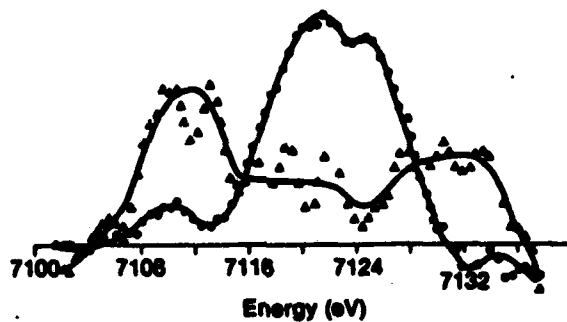


Fig. 3. Derivative spectra of the in situ (triangles) and of the ex situ (dots) nitrite edge spectra.

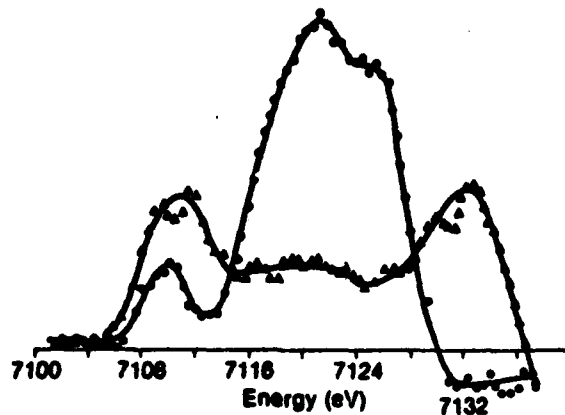


Fig. 4. Derivative spectra of the in situ (triangles) and of the ex situ (dots) chromate edge spectra.

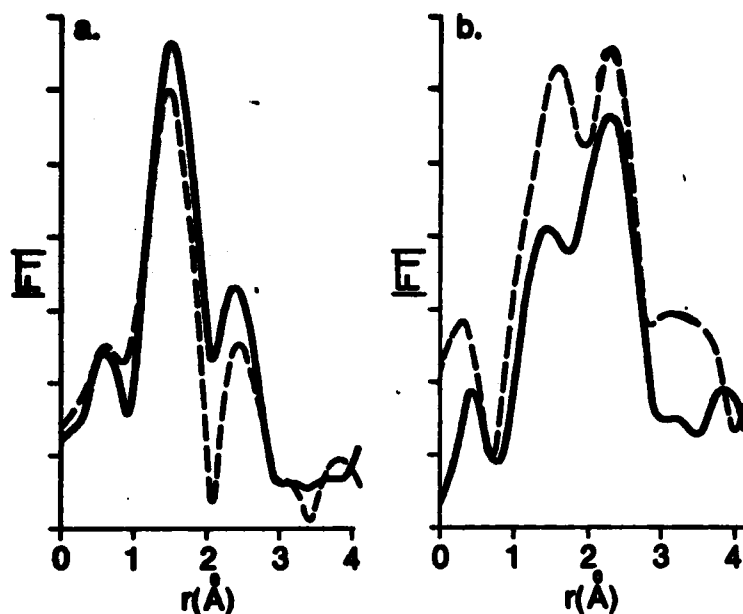


Fig. 5. Magnitudes of the Fourier transforms for the (a) ex situ and (b) in situ passive films. The nitrite film results are given by the dashed lines and the chromate film results by the solid lines.

DISCUSSION AND SUMMARY

The use of thinner iron substrates in this work yielded a clearer picture than before of the close relationship between the ex situ structures of the passive films on iron. Nevertheless, the chromate-formed structures were still found to be less well ordered than the nitrite-formed structures, and this result is interpreted as being due to the incorporation of chromium into the chromate-formed film, promoting a more glassy structure.

When the passive films were immersed in their respective passivating solutions, large differences in both the near-edge and the EXAFS spectra were observed. Both the bonding distances and the coordination are seen to change. The in situ structures, while again they are related to each other, show greater differences between their respective structures than do the pair of ex situ structures. This suggests that hydrogen containing species are part of the in situ structures, and that the influence of chromium incorporation may be greater for the in situ case. The hydrogen containing species have been suggested to appear in the structure as protons (ref. 8), water (ref. 9) or hydroxyl ions (ref. 9), through experiments involving Mossbauer spectroscopy (ref. 10), SIMS (ref. 11) and radiotracer methods (ref. 8).

The structures that produce these x-ray absorption spectra reflect the profound influence that glass formers such as chromium and additives such as hydrogen may have on the passive film on iron.

ACKNOWLEDGMENT

The contribution of J. Kruger was supported by the Office of Naval Research under contract NAONR 18-69 NRO 36-082.

REFERENCES

- 1 A. G. Revesz and J. Kruger, in Passivity of Metals, R. P. Frankenthal and J. Kruger, Eds., Electrochem Soc., Princeton, NJ (1978) 137 pp.
- 2 G. G. Long, J. Kruger, D. R. Black, and M. Kuriyama, J. Electrochem. Soc. 130 (1983) 240 pp.
- 3 G. G. Long, J. Kruger, D. R. Black, and M. Kuriyama, J. Interfacial and Electroanal. Chem., in press.
- 4 G. G. Long and M. Kuriyama, Proc. V Int'l Symposium on Passivity.
- 5 C. L. Foley, J. Kruger and C. J. Bechtoldt, J. Electrochem. Soc. 114 (1967) 994 pp.
- 6 J. Kruger, J. Electrochem. Soc. 110 (1963) 654 pp.
- 7 G. G. Long, J. Kruger, M. Kuriyama, A. I. Goldman, D. R. Black, E. Farabaugh and D. Sanders, to be published.
- 8 H. T. Yolken, J. Kruger, and J. P. Calvert, Corrosion Science 8(1968) 103 p.
- 9 T. Noda, K. Kudo and N. Sato, Z. Phys. Chem. N. F., 98 (1975) 271 pp.
- 10 W. F. O'Grady, J. Electrochem Soc., 127 (1980) 555 pp.
- 11 D. J. Murphy, J. O'M. Bockris, T. E. Pou, D. L. Cocke, and G. Sparrow, J. Electrochem. Soc. 129 (1982) 2149 pp.

Part II. To be published in Proceedings 5th International Symposium
on Passivity.

**EX-SITU AND IN-SITU SAMPLE-AND-DETECTOR CHAMBERS FOR THE STUDY OF
PASSIVE FILMS USING SURFACE EXAFS**

G. G. LONG, J. KRUGER and M. KURIYAMA
Center for Materials Science, National Bureau of Standards, Washington, DC 20234

ABSTRACT

Two sample-and-detector chambers for the study of surface films on metals using x-ray absorption spectroscopy are described. Results have been obtained using both a high intensity rotating anode x-ray generator and using the Cornell High Energy Synchrotron Source (CHESS).

INTRODUCTION

The structural study of surface passive films on metals requires a high sensitivity experiment which examines the film in an environment as near as possible to that in which the real films are used. An extended x-ray absorption fine structure (EXAFS) experiment can be used to probe the near neighbor distribution in the film, and the near edge spectral features are sensitive to the electronic structure in the film. The high sensitivity to the surface signal is achieved here by having an ultrathin substrate layer and by using an innovative detection system. For the in solution (*in situ*) experiment, the x-ray fluorescence product of the K-absorption event is detected, while for the *ex situ* (but non-vacuum) experiment the total yield electron product is detected.

THE EXAFS EXPERIMENT

The x-ray absorption experiment requires that a monochromatic (i.e. ΔE of the order of 1-10 eV) x-ray beam be continuously tuned through energies from several eV below a K- or L-absorption edge to about 1000 eV on the high energy side of the edge. The basic x-ray spectrometers - to be used in EXAFS optics as "monochromators" - are divided into two classes: flat-crystal instruments and bent-crystal instruments. The flat-crystal instruments with two or more crystals generally deliver the higher resolution. The bent-crystal instrument collects and diffracts photons within an energy band pass of the incident beam and focuses them to a position on the Rowland circle. This method of monochromatization reconcentrates the beam at the exit slit of the instrument and is very efficient (ref. 1).

EX SITU X-RAY ABSORPTION DETECTOR

A high-pass photocathode x-ray ionization chamber, especially designed for surface EXAFS (refs. 2 and 3) was adapted for structural studies of passive films on metals. The sample, of which less than 10% may be the substrate metal or alloy, serves as the conducting cathode plate inside the helium filled detector. A filter assembly in front of the detector limits the energy band pass of the detector to the region between the absorption edge of the photocathode and that of the filter. This means, for example, that an iron K-edge absorption experiment would make use of a cobalt filter, so that the high bandpass of the detector would be between 7.1 and 7.7 keV.

A schematic of the sample-and-detector chamber is shown in Fig. 1. The x-rays enter through an aluminized mylar window and impinge on the sample (which is also the photocathode) at grazing incidence. The photocathode plate absorbs the x-rays and emits electrons, which are amplified through field intensified ionization in the helium gas. The current passing through the detector is measured by an electrometer connected to the plate. The result is an experiment similar to total yield spectroscopy in which the electrons are collected as a function of the energy of the incident x-ray beam.

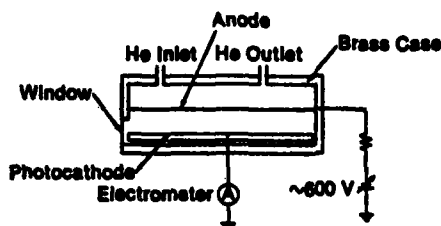


Fig. 1 The ex situ EXAFS detector and sample chamber.

Four kinds of electrons emerge from the photocathode; photoelectrons, secondaries, inelastically scattered electrons, and Auger electrons. The photoelectrons are excited simultaneously with the absorption of the x-rays, but the kinetic energy of these electrons near the absorption edge is very low, and thus they will not be able to produce much detector current. The secondary electrons that have been excited by collisions, or the inelastic electrons that are photo- or Auger electrons that have suffered inelastic collisions, have a wide spectrum of energies. The Auger electrons are emitted by the decay of the core hole states created by the photoabsorption. These electrons have large kinetic energies. The subsequent decay of the L shell holes is usually

dominated by Auger emission so that it is possible that nearly one electron may be excited for each photon absorbed.

The electrons generated near the surface of the cathode undergo field intensified ionization, increasing the current by a multiplying factor. Further sensitivity is achieved in that this detector collects over nearly the entire 2π steradian hemisphere. Using a 12 kW laboratory x-ray generator, focusing optics (ref. 1) and the present detector, the thin film EXAFS spectra of passive films shown in Fig. 2 were each obtained in the approximately 4 hours of scanning. The magnitudes of the Fourier transforms of these data are given in Fig. 3.

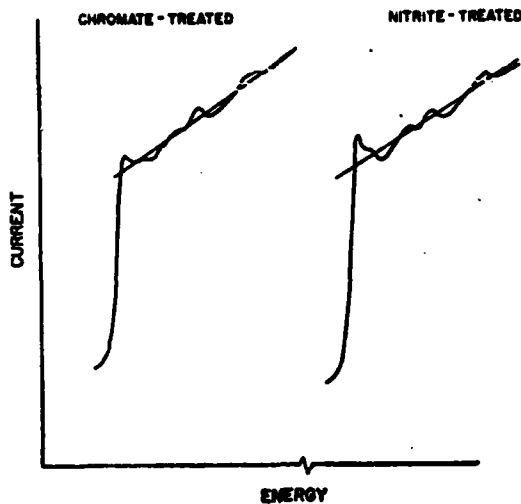


Fig. 2 EXAFS spectra of the films formed in each of two passivating solutions.

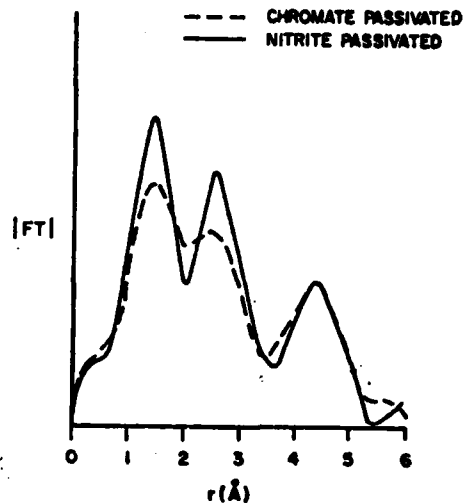


Fig. 3 Magnitude of the Fourier transforms for the data shown in Fig. 2.

IN SITU X-RAY ABSORPTION CELL

The in situ EXAFS measurement requires that the x-ray absorption spectra be taken while the thin film is immersed in an aqueous solution where electrochemical studies are performed. Fortunately, water becomes transparent again in the hard x-ray region of the electromagnetic spectrum. In this case, the x-ray absorption event is followed by measuring the photon fluorescence product of the decay of the core hole. Data collection is somewhat hampered by a large scattering component from the solution. This is brought under control through the use of an x-ray filter assembly in front of each x-ray detector, so that the signal is dominated by the fluorescence photons.

A schematic of the cell is shown in Fig. 4. All of the elements of the cell are embedded in an inert epoxy so that the surface of the film under investigation can be brought nearly into contact with the x-ray window. The reference electrode is connected to a Luggin capillary embedded in the epoxy with its opening in the plane of the specimen. The Pt counter electrode also lies in the same plane of the specimen and is connected through the epoxy to the rear of the cell. The metal sample is deposited on the surface of a glass slide and connection is made through a plug of bulk metal through the glass.

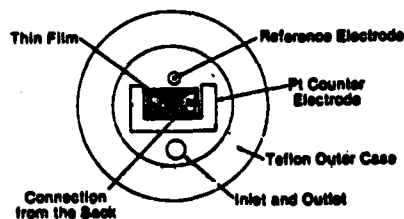


Fig. 4 The in situ EXAFS cell.

It is desirable to do the electrochemistry in a rather larger volume of solution, so the entire cell is mounted in a piston arrangement in a teflon outer case. This permits us to reduce the "as received" sample and grow the film on a bare metal surface in a large volume of solution. Once the film has formed, the current is very small, and the sample can safely be brought to within a small fraction of a mm of the x-ray window for measurement while under potentiostatic control.

The cell was tested to demonstrate that a passive film could be formed and maintained under anodic polarization. The cell was also tested to demonstrate that spectra could be obtained through the x-ray window and the aqueous electrolyte. In situ and ex situ data were taken using the C-1 monochromator at CHESS. Fig. 5 shows the magnitude of the Fourier transform for the (a) ex situ and (b) in situ data, both taken in high resolution geometry. Fig. 5(a) is to be compared with Fig. 3 which was derived from laboratory data using the ex situ detector. Data collection times were similar.

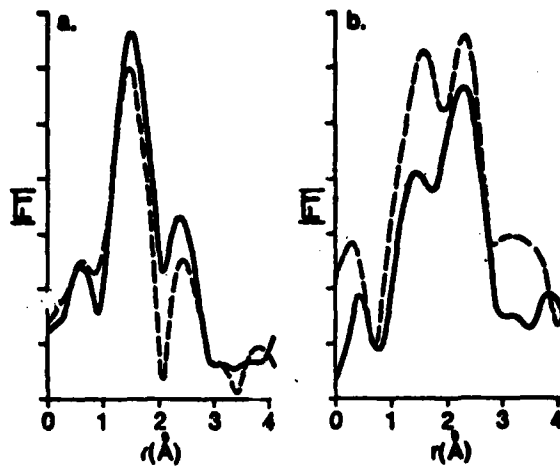


Fig. 5 Magnitudes of the Fourier transforms for the (a) ex situ and (b) in situ passive films. The nitrite-formed film results are given by the dashed lines and the chromate-formed film results by the solid lines.

REFERENCES

- 1 G. G. Cohen, D. A. Fischer, J. Colbert and N. J. Shevchik, Rev. Sci. Instrum. 51 (1980) 273 pp.
- 2 N. J. Shevchik and D. A. Fischer, Rev. Sci. Instrum. 50 (1979) 577 pp.
- 3 D. A. Fischer, G. G. Cohen and N. J. Shevchik, J. Phys. F 10 (1980) L139 pp.

Part III. To be submitted to Journal of Coatings Technology.

Ellipsometric Studies of Chelating Inhibitor Effects on the
Cathodic Delamination of an Organic Coating on Iron

J. J. Ritter
Inorganic Materials Division
Center for Materials Science
National Bureau of Standards
Washington, D.C. 20234

ABSTRACT

Qualitative ellipsometry has been used to study the effects of chelating inhibitors on the cathodic delamination of an acrylic coating from an iron surface. The chelating inhibitors 8-hydroxyquinoline (8-HQ) and 2,5 dimercapto 1,3,4 thiadiazole (DMTDA), when dispersed in the coating were observed to delay the onset of delamination. Catechol was found to be an ineffective inhibitor. A similar beneficial effect was noted with a two-layer system employing a zinc chromate primer. However, when 8-HQ and DMTDA were applied by an anodic pretreatment procedure they were relatively ineffective, whereas 4-methylcatechol similarly applied, exhibited impressive inhibition.

Ellipsometric Studies of Chelating Inhibitor Effects on the Cathodic Delamination of an Organic Coating on Iron

J. J. Ritter
Inorganic Materials Division
Center for Materials Science
National Bureau of Standards
Washington, D.C. 20234

INTRODUCTION

Previous publications from our laboratories have shown the effectiveness of qualitative ellipsometry in the study of interfacial cathodic events during the corrosion of painted metal surfaces.¹⁻⁴ Since coatings bond to the metal oxide films, and since many corrosion inhibitors seem to function at or within this interfacial metal oxide film, it seemed a natural extension of our previous work to examine the effects of corrosion inhibiting species on cathodic delamination. While many paint systems in service presently rely heavily on inorganic species to achieve inhibition, an active search for substitute materials goes on to obtain more effective inhibition, reduce costs, meet environmental standards, and minimize the consumption of strategic metals.

We selected a small group of organic molecules with a potential for forming coordination complexes with iron. The effectiveness of these types of chelating molecules in corrosion inhibition has been described previously by other investigators.⁵⁻⁶

The present work will describe the cathodic delamination behavior of acrylic coated iron where chelating inhibitors have been supplied in two different ways. In the first method, the inhibitor is homogeneously dispersed within the coating; while, in the second method, the inhibitor is applied in a two step anodization process, as recently described by

Leidheiser et al.⁷ An acrylic coating is applied over this pretreated surface.

EXPERIMENTAL

Iron specimens were mounted in epoxy and finished on a series of SiC papers of 320, 400, and 600 grit. Final polishing was accomplished with 6.0, 1.0, and 0.05 μm abrasives.

A clear, proprietary acrylic coating material was dissolved in toluene and specimens coated by dipping. The chelating inhibitors employed and their structural formulae are given in Fig. 1. Chelating inhibitors were dispersed in the coating material in the 1 to 2 percent range by first dissolving the inhibitor in toluene and then using this toluene as the solvent to prepare the coating medium. The two layer, nine percent zinc chromate primer system shown in Fig. 2 was prepared by pressing a 6.0 mm dia. polytetrafluoroethylene cylinder to the center of the metal surface and applying the proprietary primer by brushing. After the primer had cured, the PTFE mask was removed, and the clear acrylic topcoat was applied by dipping. The 6.0 mm view of the metal surface through the clear acrylic provided the necessary observation "window" for the ellipsometric experiments on this specimen.

The two step anodization procedure for the applications of chelating inhibitors was adapted from the method described by Leidheiser et al.⁷ The method is summarized as follows. An uncoated, mounted iron specimen is aligned in the ellipsometer cell and submerged in 170 ml pH 8.4 borate buffer solution. The solution is deaerated with N_2 and the specimen is observed ellipsometrically under open circuit conditions for ~ 1.0 h. An anodic film is grown on the metal surface with an impressed voltage of 1.2 V S.C.E. After ~ 10 min of anodization, 50 ml

of borate buffer containing a quantity of chelating material calculated to give $\sim 10^{-4}$ M chelate concentration in the total solution is added. Rapid mixing is effected by the continuing N_2 flow, and the potential was held at 1.2 V S.C.E. until the inhibitor layer is well developed. The layered structure is shown schematically in Fig. 3. The specimen is removed from the cell, rinsed with water, dried with an air jet, and coated with acrylic by dipping. Typical coating cure times were 24 h at 25 °C.

The corrosion of all coated specimens was conducted in 0.05 M NaCl at 25 °C. Typically, the coated specimens were observed for 400 to 500 min. before the corrosion process was initiated by puncturing the coating ~ 0.5 cm from the ellipsometric observation region, as shown in Fig. 2. Ellipsometric data were acquired at a rate of one set of points per minute, under computer control.

Interpretation of Ellipsometric Behavior for the Iron/Acrylic System

For comparison purposes, a typical ellipsometric response curve for acrylic coated iron undergoing corrosion in 0.05 M NaCl is shown in Fig. 4. A detailed interpretation of this type of response has been given previously,⁴ but a brief summary is provided here. Previous observations on uncoated iron systems under potential control in either borate buffer solutions or in saturated NaOH solutions indicate qualitatively that simultaneous changes in the Δ and ψ parameters in opposite directions is indicative of a changes in the metal oxide film thickness. A simultaneous change of Δ and ψ in the same direction is indicative of a surface texture change; i.e., surface roughening or smoothing. The coating on the system shown in Fig. 4 was punctured at $t = 0$. At about 500 min, the Δ signal rises while the ψ signal simultaneously declines. These

changes are interpreted as a thinning of the interfacial oxide film on the basis of our ellipsometer observations on uncoated iron in a controlled environment. Cathodic regions under coatings are known to become highly alkaline.¹⁻³ In earlier work,⁴ we have shown that native oxide films on iron will dissolve (i.e., become thinner) in highly alkaline media. Since the puncture site is the focus of anodic activity, cathodic sites develop elsewhere under the coating, eventually reaching the region being observed ellipsometrically. Thus, the observed mode of delamination for the system shown in Fig. 4 is the chemical dissolution of the interfacial oxide film. Subsequent ellipsometric changes show events such as surface roughening and reprecipitation of dissolved iron species as indicated on Fig. 4. Experience gained from experiments stopped soon after surface roughening is detected ellipsometrically indicates almost invariably that the coating can be readily detached with forceps. This evidence leads us to assert that surface roughening is a post-delamination event. Thus, the ellipsometrically detected onset of surface roughening can be used as an indicator for the failure of the coating in the ellipsometrically monitored region of the specimen.

RESULTS AND DISCUSSION

Iron/Acrylic System with Coating Dispersed Inhibitors

Catechol

Figure 5 shows the ellipsometric responses for the iron/acrylic/catechol system. The vertical arrow (+) in this figure and in subsequent figures marks the time at which the coating was punctured. Note that the ellipsometric activity prior to puncture suggests possible subcoating development of an inhibitor film (Δ declines, ψ rises). However, within

about 100 min after puncture, surface roughening is indicated (Δ and ψ decline in concert). Obviously, catechol provides no inhibition; and, in fact, when compared to the post-puncture time scale in Fig. 4, may actually accelerate the delamination process. This result is not surprising, since catechol reportedly offers little protection to iron systems.⁵

2,5 dimercapto-1,3,4 thiadiazole (DMTDA)

Figure 6 shows the ellipsometric responses for the iron/acrylic system with DMTDA dispersed in the coating. The pre-puncture signals suggest changes in surface texture (probably surface smoothing) as the inhibitor interacts in the interfacial region. After the coating is punctured, the onset of delamination is delayed nearly 1800 min, whereas, in the uninhibited system (Fig. 4), delamination is typically seen within 500 minutes. Note also, that Δ and ψ initially decline in concert, indicating that delamination has occurred just previously, and surface roughening has set in. In comparing this behavior to that seen in Fig. 4, the lack of initial rise in Δ is interpreted as delamination having occurred by a mechanism other than oxide film dissolution. The presence of the inhibitor has not only delayed the onset of delamination, but has probably also altered the mode of delamination.

8-hydroxyquinoline (8-HQ)

Figure 7 shows the case for inhibition by 8-hydroxyquinoline. Note very little pre-puncture activity but that Δ and ψ converge very slowly after the coating is damaged. This convergence is interpreted as the development of an interfacial chelate layer. Finally, after \sim 5000 minutes, delamination sets in with a probable initial chemical destruction of the chelate/oxide interface, followed by the expected surface rough-

ening phenomenon. This inhibitor delays the onset of delamination but probably does not alter the mechanism.

Zinc Chromate Primer/Acrylic System

For comparison purposes, the zinc chromate primer/acrylic topcoat system was studied under comparable conditions. Figure 8 shows a decline in Δ and a very slight rise in ψ , suggesting a possible ingress of chromate into the interfacial region. Delamination is delayed by about 5000 min; a performance rather comparable to that of 8-hydroxyquinoline. Note that when the large ellipsometric changes occur, Δ and ψ move in concert, signifying the onset of surface roughening without preceding oxide dissolution; i.e., Δ and ψ do not show an initial divergence, as in Fig. 4. Thus, in this system, delamination is delayed and probably occurs by some mechanism other than that of oxide dissolution.

Inhibitor Application During Anodization

Leidheiser and co-workers at Lehigh University have recently developed a two step anodization process for the application of chelating inhibitors to uncoated surfaces.⁷ This work has prompted us to examine this procedure ellipsometrically and also study the corrosion performance of coated samples which had been subjected to this method of inhibitor application.

Ellipsometric Changes During the Two Step Anodization

Figure 9 shows, initially, the stable ellipsometric response for uncoated iron at open circuit potential in borate buffer solution. At $t \sim 50$ min, a potential of +1.2 V S.C.E. was applied to the specimen. Delta declines sharply, ψ rises slightly but measurably. These changes signify the growth of an anodic film on top of the existing native oxide

film. At $t \sim 65$ min, the potential being held at +1.2 V S.C.E., 8-hydroxyquinoline was added to the solution. Δ and ψ changes indicate the growth of about 10 nm of additional film, presumably incorporating the chelating inhibitor.

Figure 10 shows the somewhat more complex behavior of DMTDA application with this procedure. The initial anodization at $t \sim 120$ min proceeds as noted earlier. However, upon the addition of DMTDA, film growth is followed by surface smoothing and then by surface roughening before a stable situation is achieved at $t \sim 150$ min. The final disposition of Δ and ψ values beyond 150 min suggest that some chelate film is probably present, although the preceding surface texture changes (i.e., the smoothing and roughening) render the estimation of its thickness difficult.

A third case of inhibitor application by two step anodization is shown in Fig. 11. The early behavior of the specimen at open circuit and anodization is similar to the preceding two examples. However, the addition of 4-methyl catechol produces only a small gradual change in Δ and a very noticeable jump in ψ . These changes are interpreted to arise from the growth of a rather thin (one monolayer or less) chelate film.

Thus, in the application of different inhibitors by the two step anodization process, we have observed very diverse modes of surface modification, including the formation of thick films, surface texture changes, and the growth of thin films.

The Effects of Two Step Anodization Pretreatment on the Corrosion of Coated Iron

Figures 12 and 13 show the respective performances of the acrylic coating over 8-HQ and DMTDA pretreated surfaces. In each case, delamination is seen within a few hundred minutes after the coatings are

damaged, as evidenced by the early large changes in Δ and ψ . In the case of the 8-HQ treated surface (Fig. 12), the delamination appears to be due to some dissolution of the anodic film, since Δ and ψ initially move in opposing directions. This detail is not seen in the case for DMTDA (Fig. 13) and suggests that a different delamination mechanism may be operative. The case for the specimen anodized in the presence of 4-MC (Fig. 14) is particularly interesting when compared to the other inhibitors studied. Note that, from $t = 0$ to $t \sim 4800$ min, Δ and ψ show a concerted decline of only a few degrees, suggesting rather minor surface texture changes. At about 4800 minutes, Δ begins to increase slowly, while ψ continues to decline, suggesting a very gradual dissolution of the anodized layer and a concomitant gradual delamination. Indeed, at the termination of this experiment at 9000 minutes, the coating was found to be rather well adhered to the specimen surface. In contrast, the coatings on the 8-HQ and DMTDA pretreated systems could be easily detached from the substrate after only 6000 minutes.

SUMMARY

For the iron/acrylic system studied, chelating inhibitors homogeneously dispersed in the coating affect the coating failure process by delaying the onset of delamination and/or altering the mechanism of delamination. DMTDA and 8-HQ are effective in delaying coating failure, whereas catechol is not. Comparable results for inhibition have been obtained with a zinc chromate primer/acrylic topcoat system. Our ellipsometric observations on the deposition of different chelating inhibitors during a two step anodization have shown a wide range of behaviors, including the formation of relatively thick deposits, metal dissolution, and the deposition of near-monolayer films. DMTDA and 8-HQ are not

effective inhibitors when anodically applied, whereas good results were obtained with 4-MC.

Thus, our results indicate that, for a given coating system, both the method of chelating inhibitor introduction and its chemical nature can affect its performance in retarding coating failure.

ACKNOWLEDGEMENTS

The author would like to thank Dr. J. Kruger, NBS, for encouragement and many useful suggestions. This work was partially funded by the Office of Naval Research, under contract number NAONR 18-69 NRO 36-082.

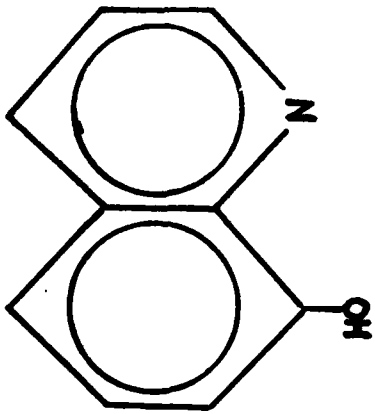
REFERENCES

1. Ritter, J. J. and Kruger, J., Surf. Sci., 96, 364 (1980).
2. Ritter, J. J. and Kruger, J., "Corrosion Control by Organic Coatings", Henry Leidheiser, Jr., ed., Ntl. Assoc. Corr. Eng., Houston, TX (1981) p. 28.
3. Ritter, J. J. and Rodriguez, M. J., Corrosion, 38, 223 (1982).
4. Ritter, J. J., J. Coatings Tech., 54, 51 (1982).
5. Weisstuch, A.; Carter, D. A.; and Nathan, C. C., Matls. Protection & Performance, 10, 11 (1971).
6. Riggs; Olen, L., Jr., "Corrosion Inhibitors", C. C. Nathan, ed., Ntl. Assoc. Corr. Eng., Houston, TX (1973).
7. Leidheiser, H., Jr. and Konno, H., J. Electrochem. Soc. (1983).

FIGURE CAPTIONS

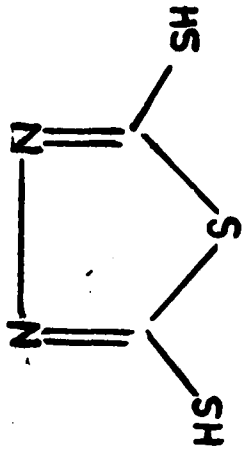
1. Structural formulae for the chelating inhibitors.
2. Proposed layered structure for specimen pretreated with an inhibitor in a two-step anodization process.
3. Cutaway view of the specimen arrangement used for the zinc chromate primer/acrylic topcoat system.
4. Typical ellipsometric response curve for an acrylic-coated iron specimen undergoing corrosion in dilute NaCl solution.
5. Ellipsometric responses for corrosion in the iron/acrylic system with 1.4 percent catechol dispersed in the acrylic coating.
6. Ellipsometric responses for corrosion in the iron/acrylic system with DMTDA dispersed in the acrylic coating.
7. Ellipsometric responses for corrosion in the iron/acrylic system with 1.7 percent 8-hydroxyquinoline dispersed in the acrylic coating.
8. Ellipsometric responses for corrosion in the iron/zinc chromate primer/acrylic topcoat system.
9. Typical ellipsometric responses for the application of 8-hydroxyquinoline in a two-step anodization procedure.
10. Typical ellipsometric responses for the application of DMTDA in a two-step anodization procedure.
11. Typical ellipsometric responses for the application of 4-methylcatechol in a two-step anodization procedure.
12. Ellipsometric responses for the iron/acrylic system undergoing corrosion where the iron surface had been pretreated with 8-HQ in a two-step anodization process.

13. Ellipsometric responses for the iron/acrylic system undergoing corrosion where the iron surface had been pretreated with DMTDA in a two-step anodization process.
14. Ellipsometric responses for the iron/acrylic system undergoing corrosion where the iron surface had been pretreated with 4-MC in a two-step anodization process.



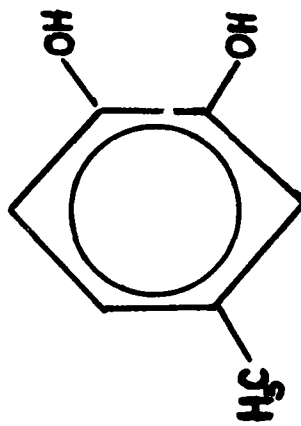
8-hydroxyquinoline

(8-HQ)



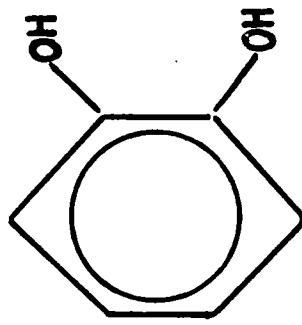
2,5 dimercapto 1,3,4 thiadiazole

(DMTDA)



4-methyl catechol

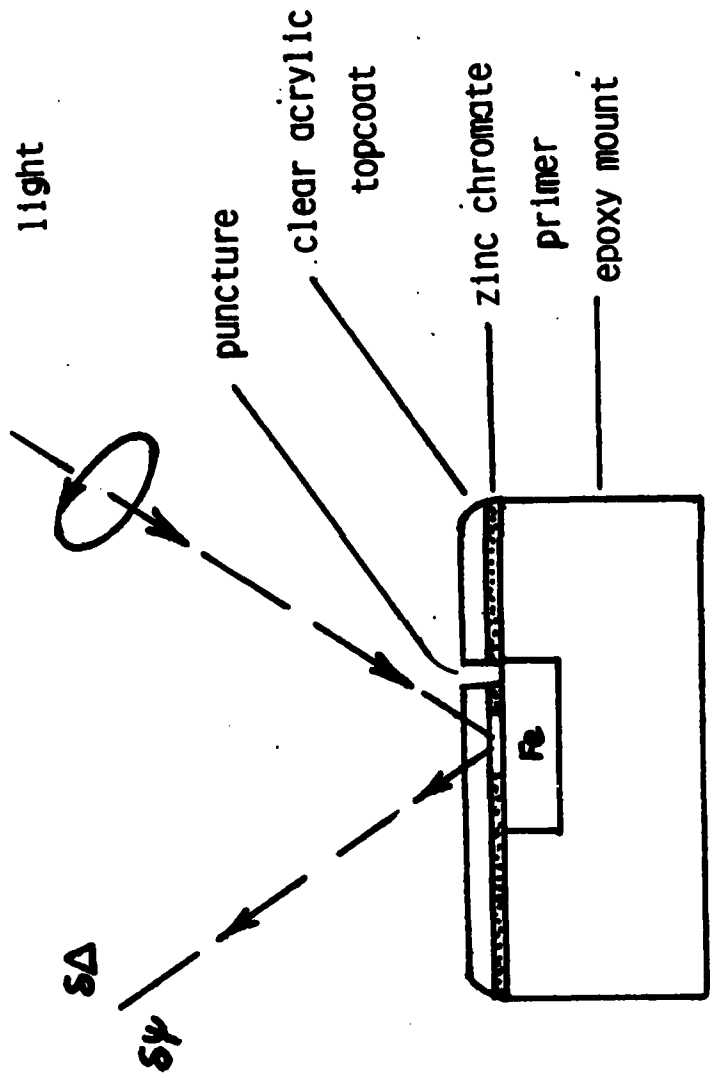
(4-MC)



catechol

elliptically polarized

light



puncture

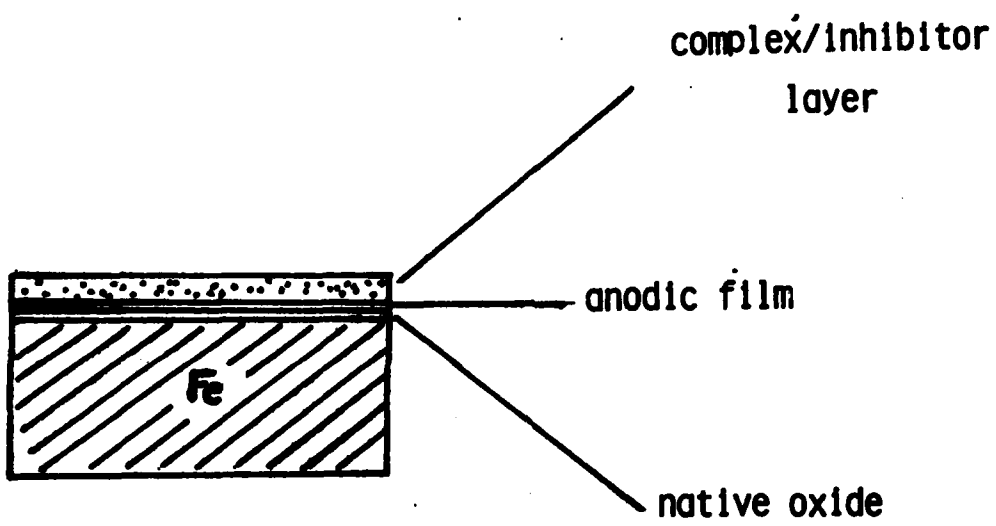
clear acrylic
topcoat

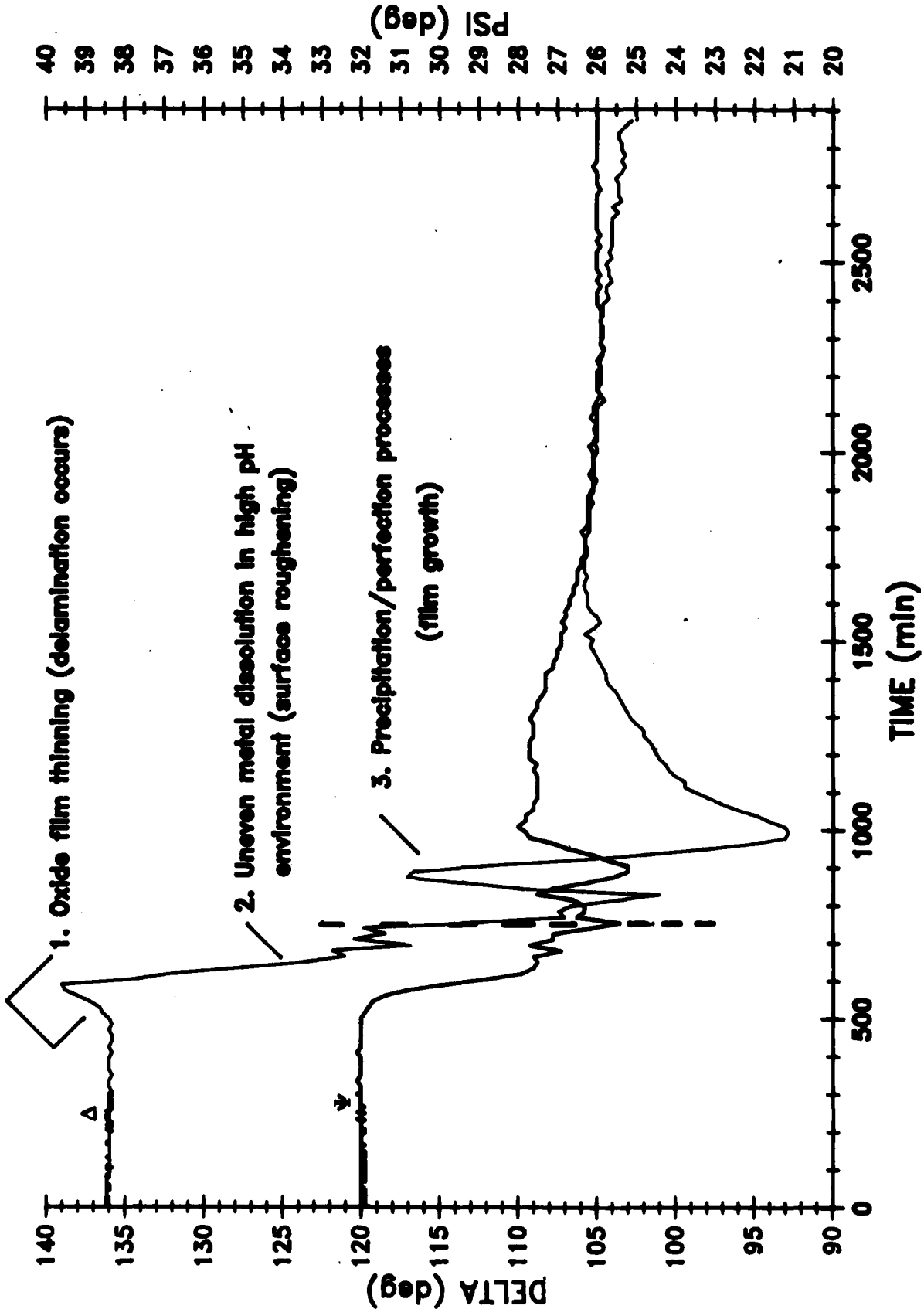
zinc chromate

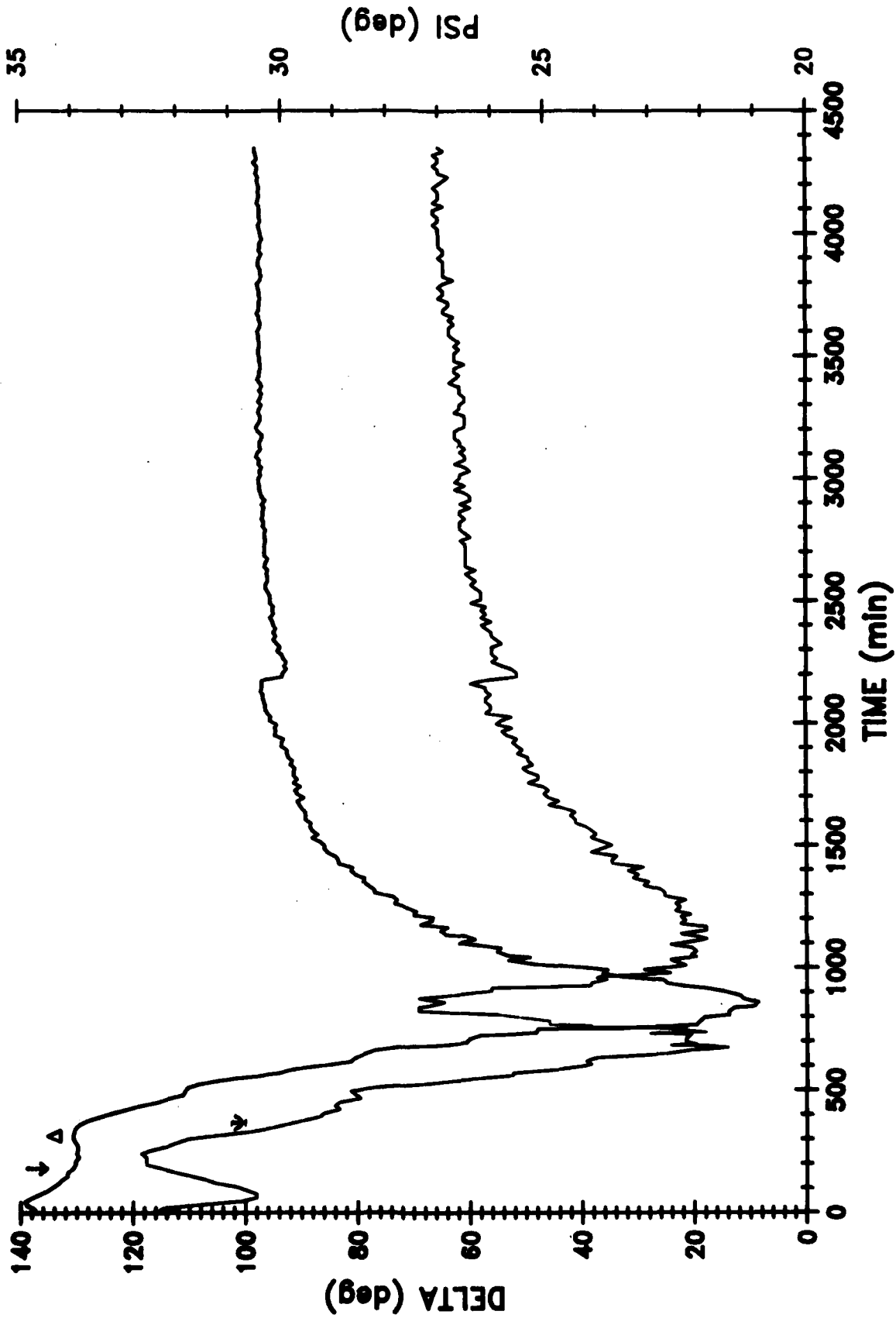
primer

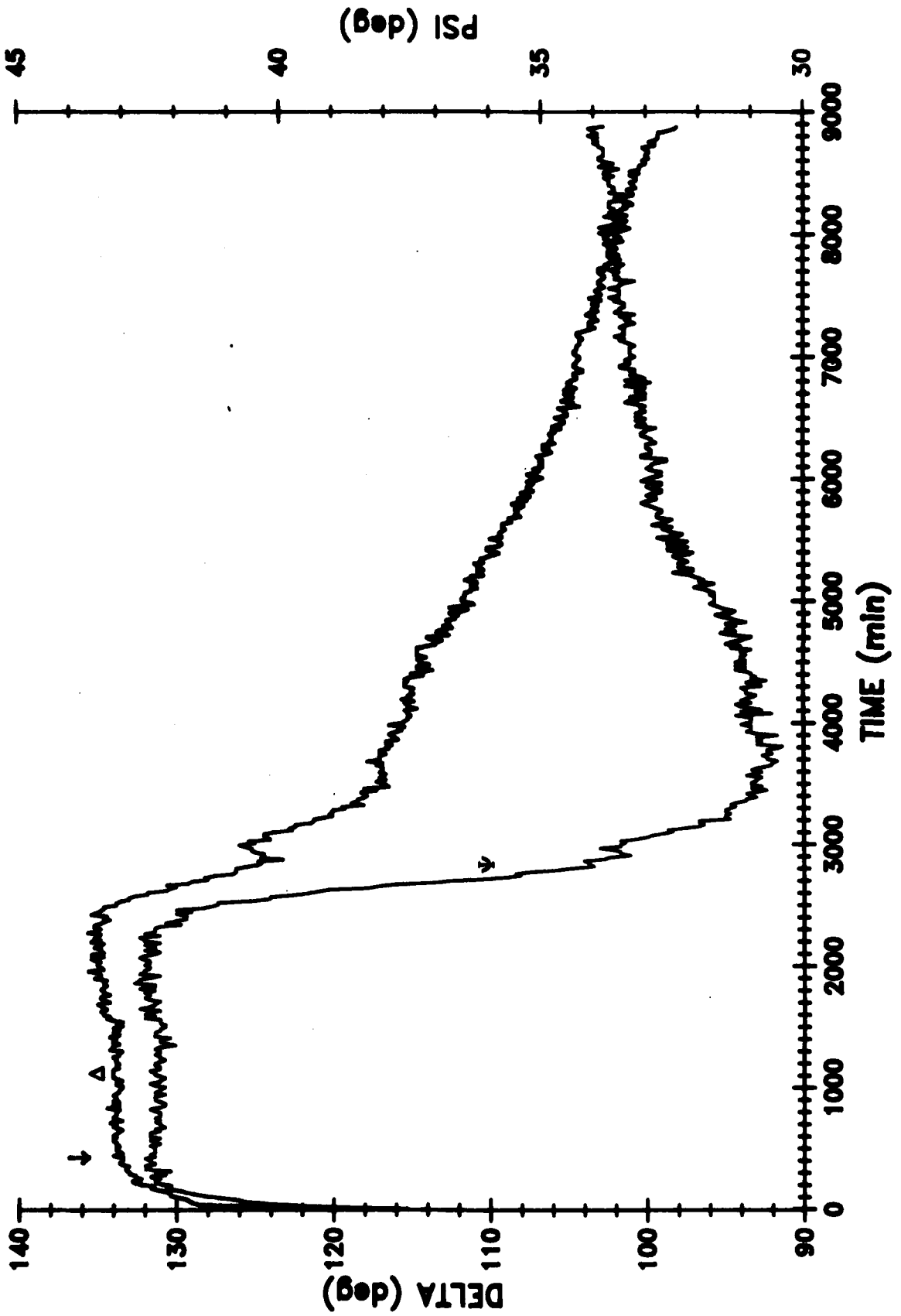
epoxy mount

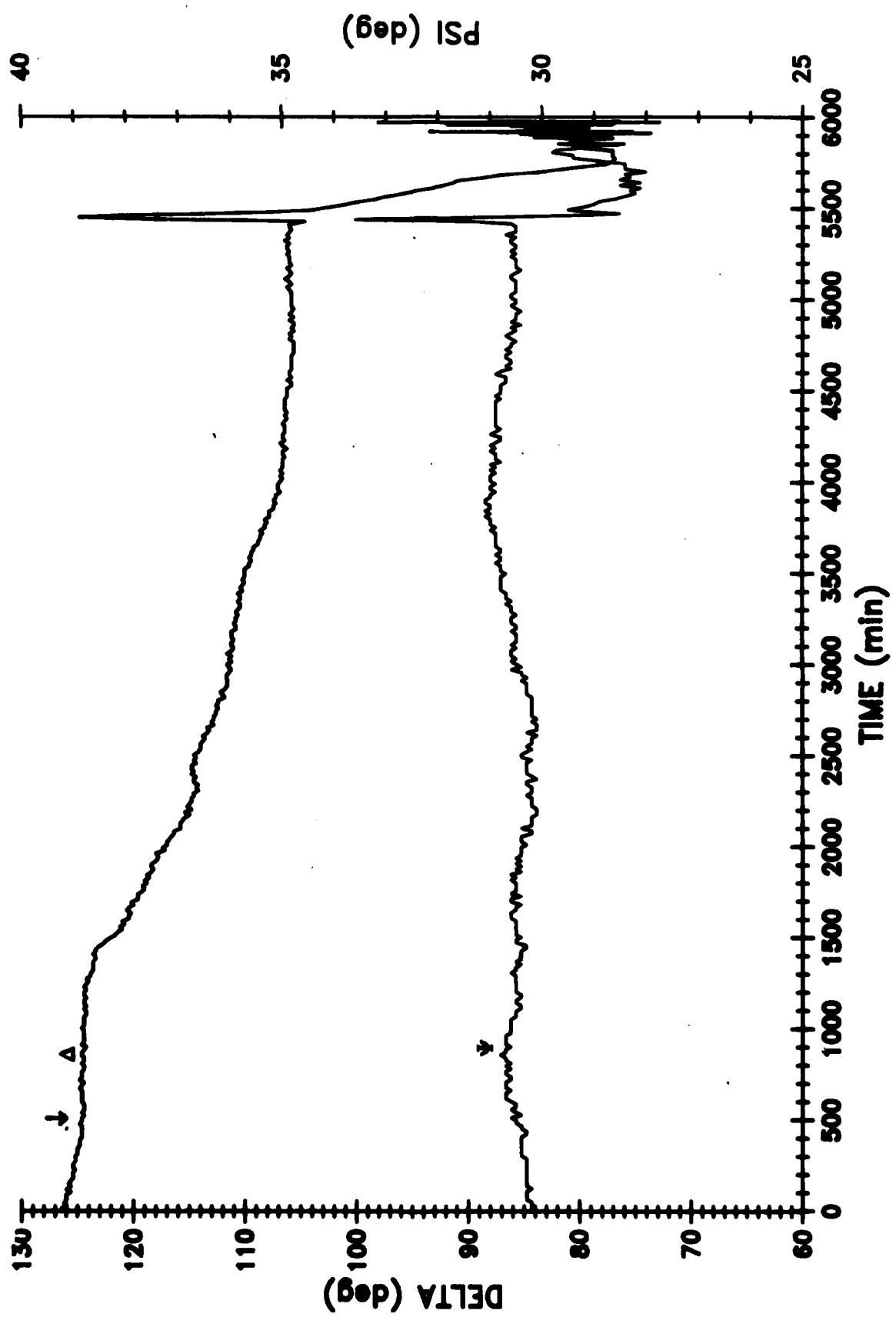
~ 0.5 cm

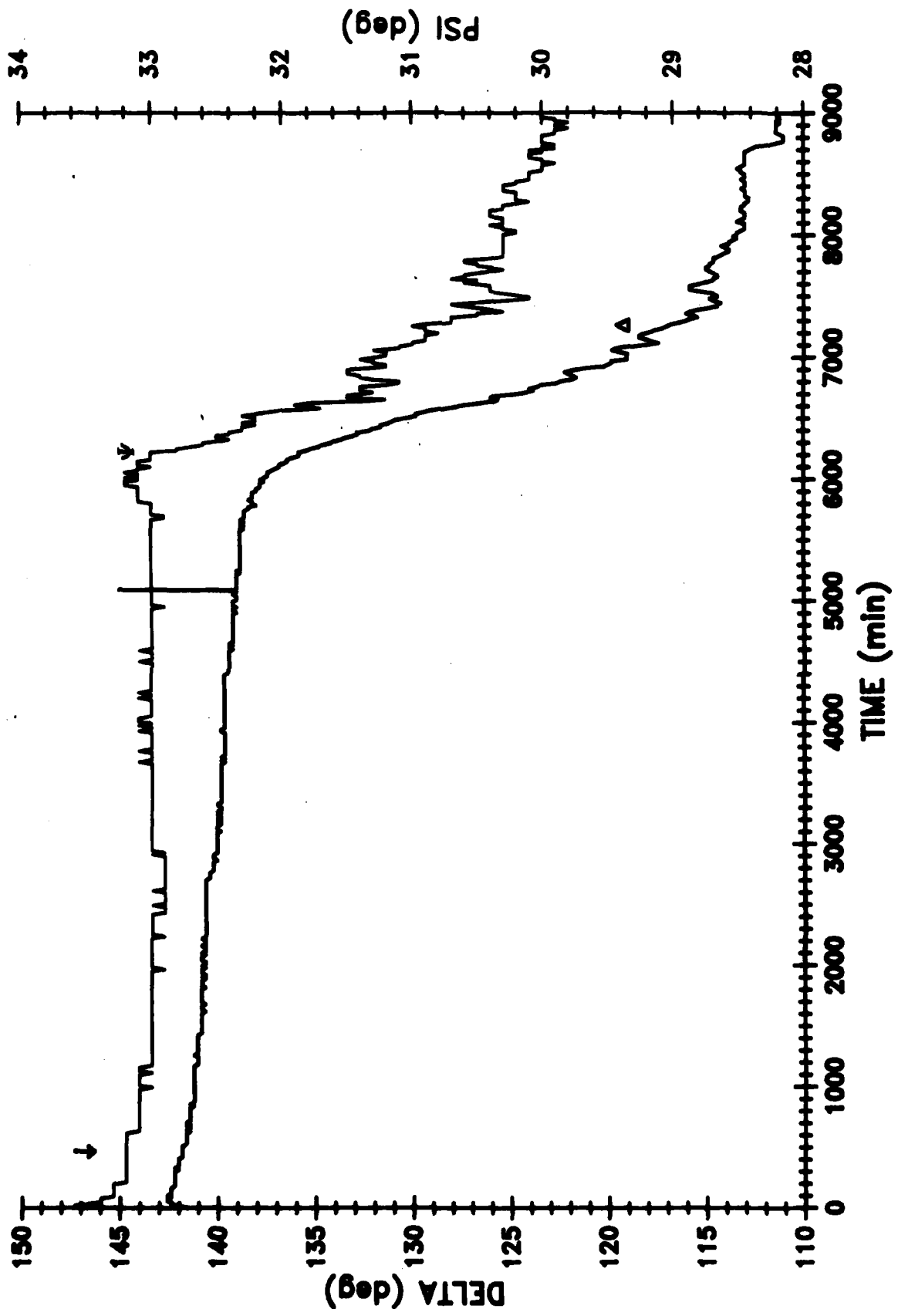


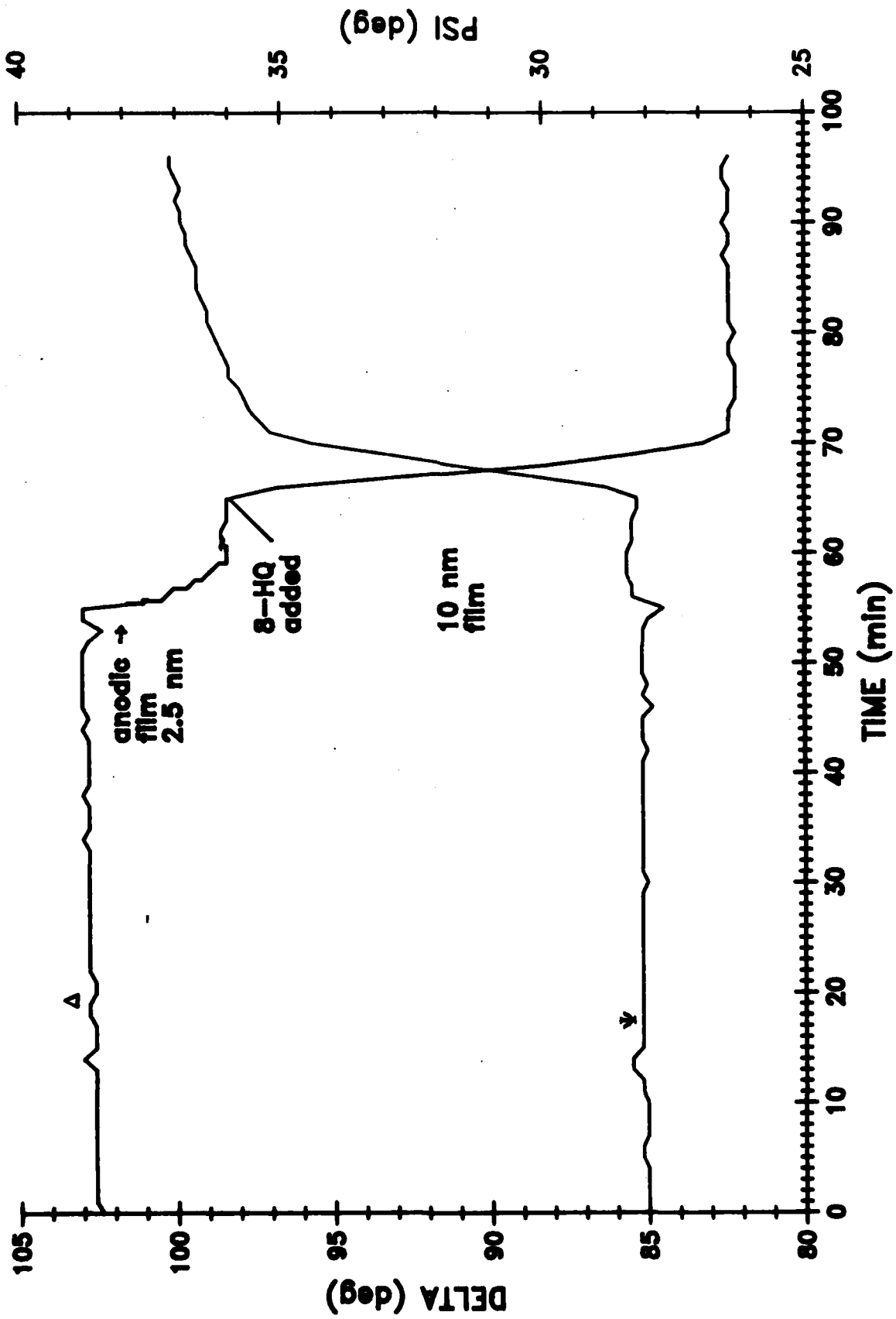


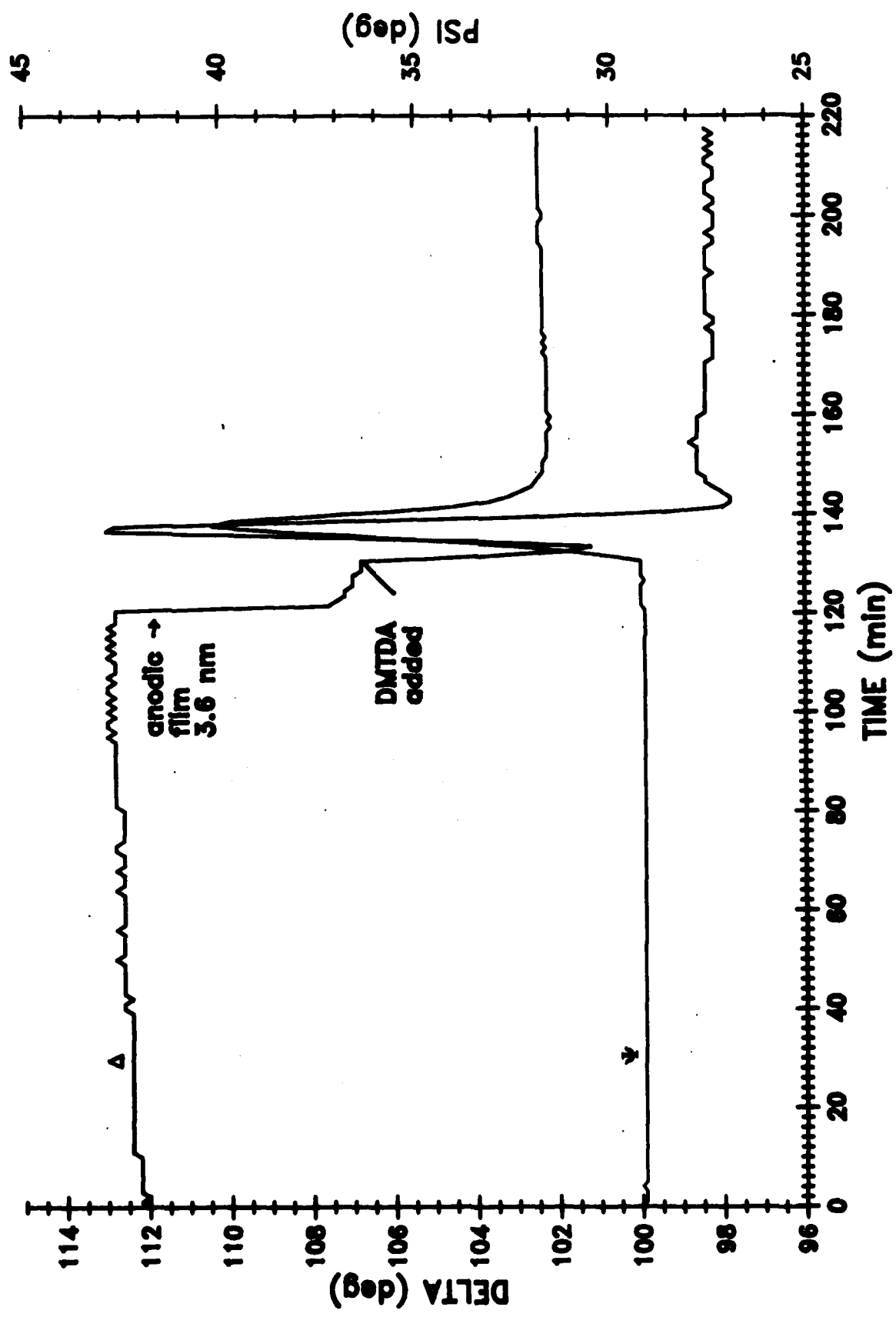


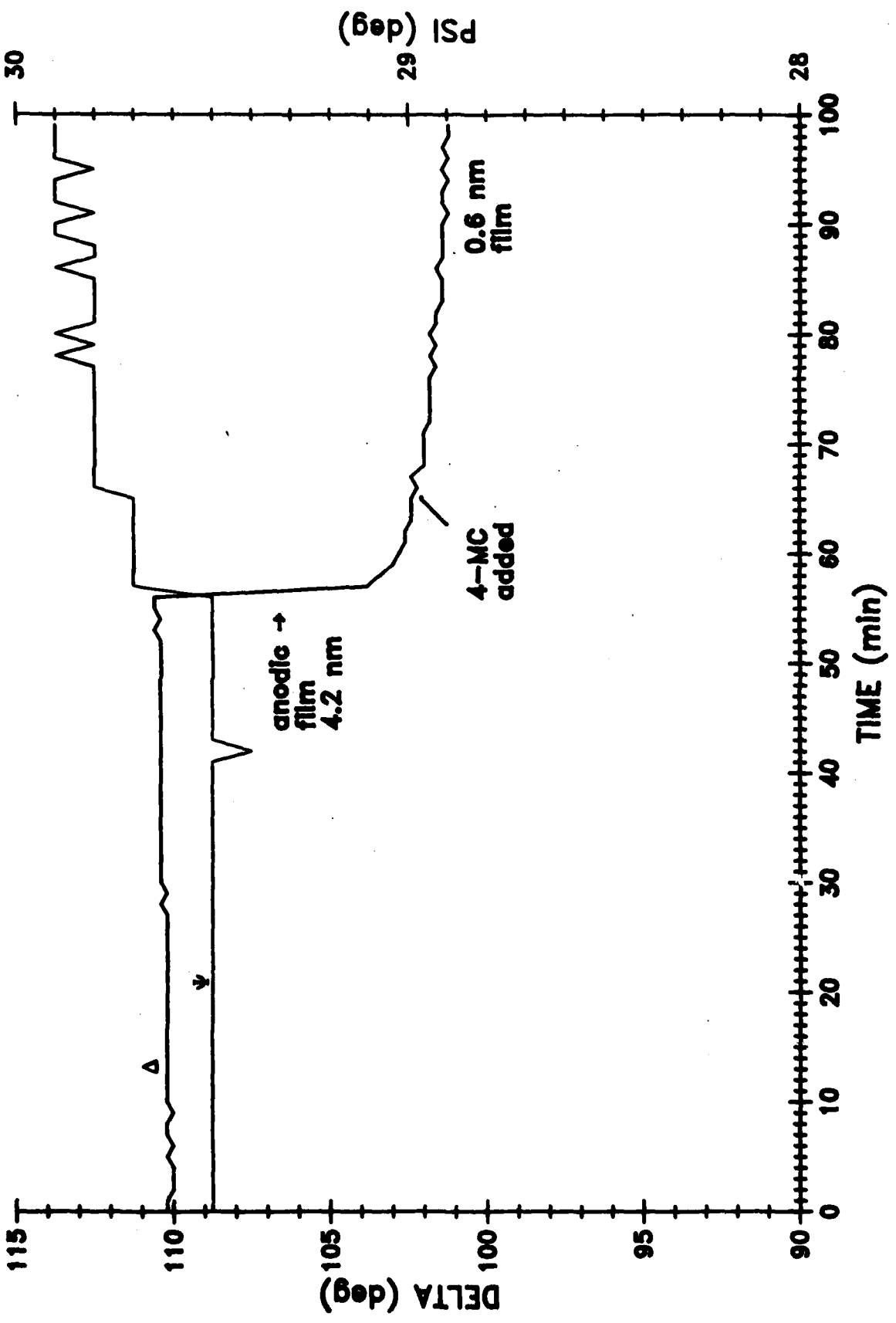


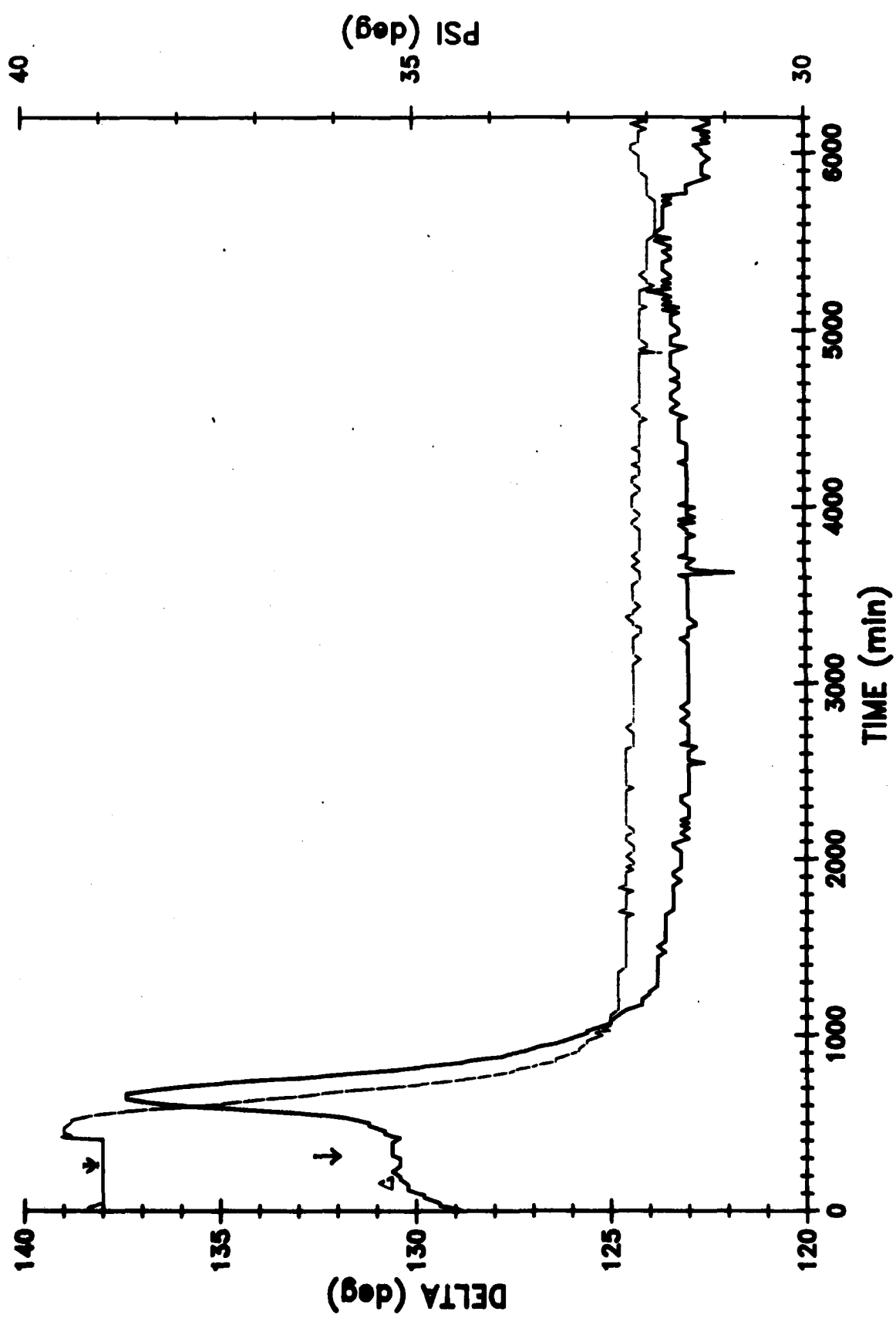


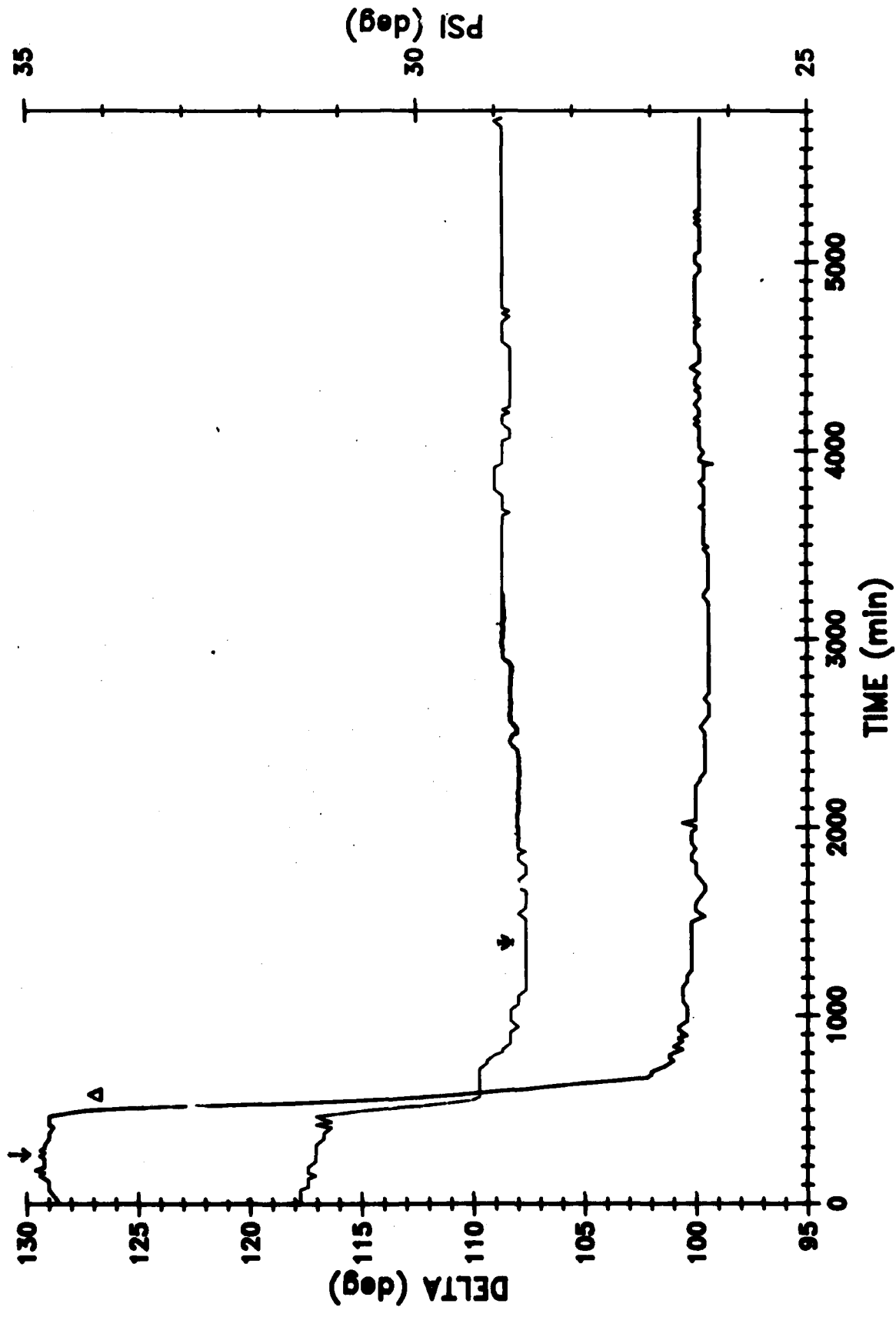


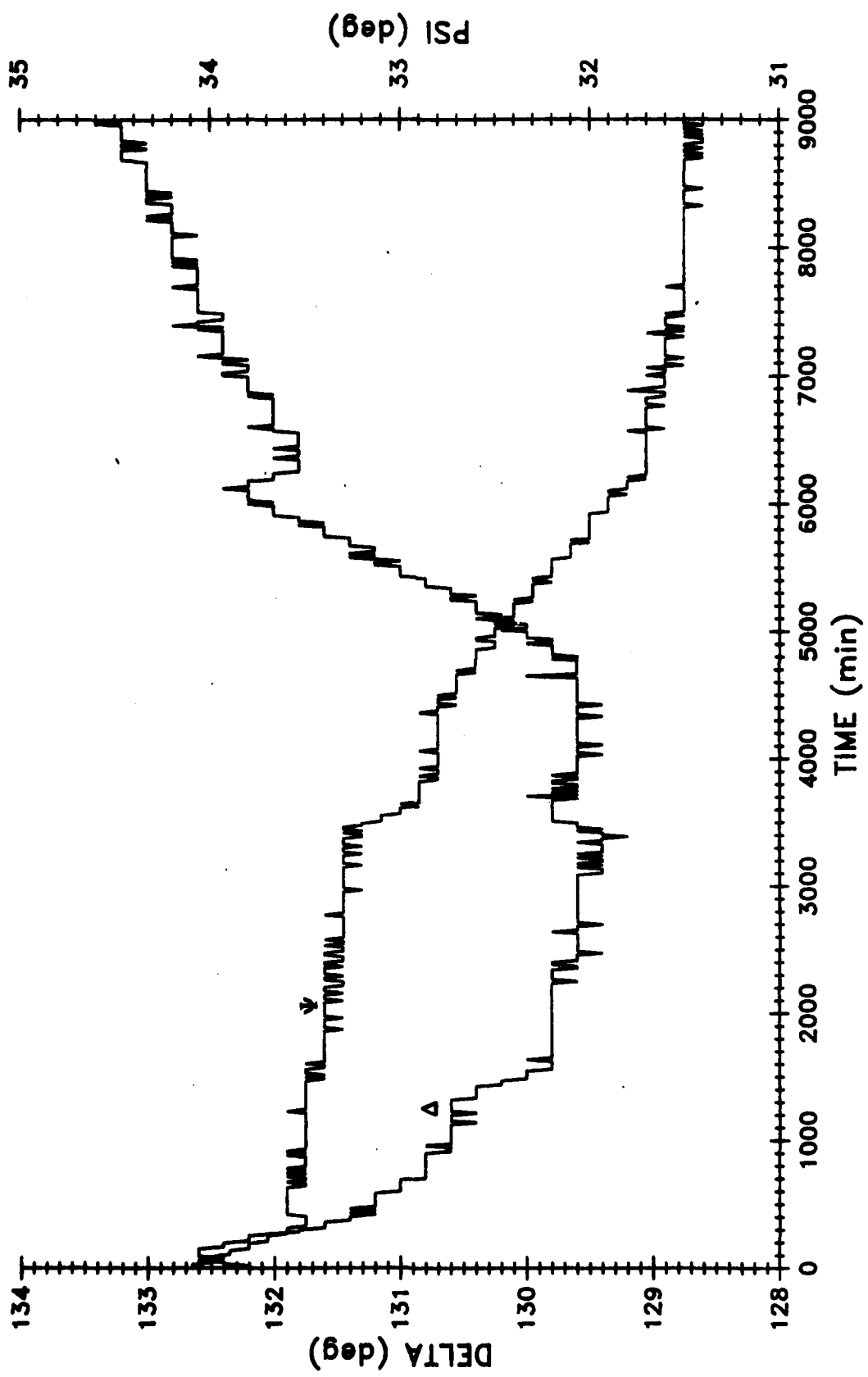












Part IV To be published in the Proceedings of International Conference
on Ellipsometry and other Optical Methods for the Analysis of
Surfaces and their Films.

Further Development of the Qualitative Ellipsometric Technique for the
Study of Corrosion Processes under Organic Coatings.

J. J. Ritter and J. Kruger
Center for Materials Science
National Bureau of Standards
Washington, DC, USA

Resumé

Le développement d'une technique ellipsométrique utilisée pour étudier les processus de corrosion sous revêtements organiques est décrite. Ce développement comprend la capacité de détecter l'influence de différents revêtements organiques, de distinguer entre l'apparition de rugosité et la croissance d'un film ou la dissolution, enfin d'étudier le processus de corrosion se produisant sur des sites anodiques et cathodiques séparés.

Abstract - We describe the further development of an ellipsometric technique used to study corrosion processes under organic coatings. These developments include the ability to (1) detect the effect of different organic coating, (2) distinguish between surface roughening and film growth or dissolution, and (3) study corrosion processes occurring on separate anodic and cathodic sites.

The qualitative ellipsometric technique developed for the study of corrosion processes under organic coatings described at the International Conference on Ellipsometry held in Berkeley, California has been refined and extended. These new developments which will be described in this paper are the following. (1) the demonstration that the ellipsometer is capable of revealing the effect of using different organic coatings; (2) the development of an ellipsometric method to distinguish between surface roughening and film growth or dissolution processes occurring under organic coatings and (3) the development of a segmented specimen technique that allows an ellipsometric study of the separate anodic and cathodic areas that form under an organic coating.

Studying the Effect of Organic Coating Type

Previous studies (1,2) applying ellipsometry to the investigation of corrosion processes under organic coating have utilized air-cured collodion (cellulose dinitrate), assuming that the nature of the transparent organic coating would not have a significant effect on the change of the ellipsometric parameters, Δ and ψ , during the early stages of the corrosion processes occurring under the coatings. As Figs. 1a and b show, this is not so. Indeed, both the nature of the polymer constituting the coating and the temperature of the cure (heat treatment) strongly influence the changes in Δ with time when the coated metal is immersed in an aqueous electrolyte. The interpretation of Fig. 1a (the air cured room temperature coatings) is given in Fig. 2 and discussed in the next section. When the coatings are cured in air at an elevated temperature (200°C), it is more difficult to give a detailed interpretation. The large rise in Δ at the beginning of the corrosion process is probably due to the dissolution of a rather thick oxide film (~14 nm) formed during the curing process of 200°C. The events beyond the initial sharp rise in Δ are more difficult to interpret. A more detailed discussion is given by Ritter /3/.

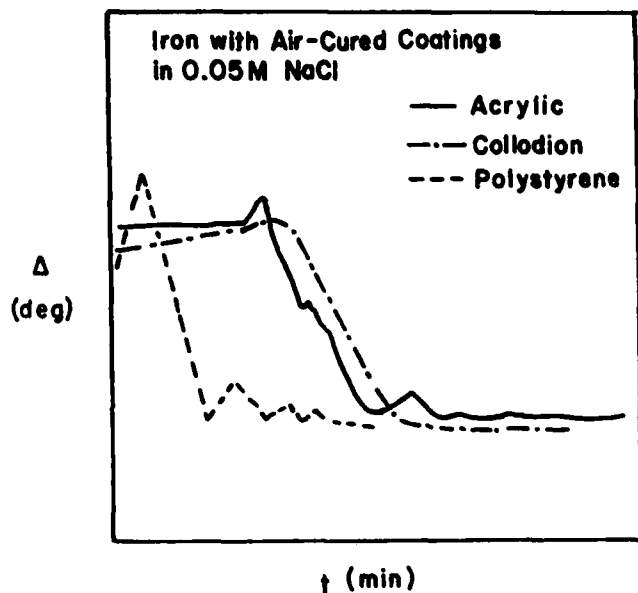


Fig. 1a - Variation of Δ with time for three iron/coating systems undergoing corrosion in an aqueous chloride solution. The coatings shown were cured in air at room temperature.

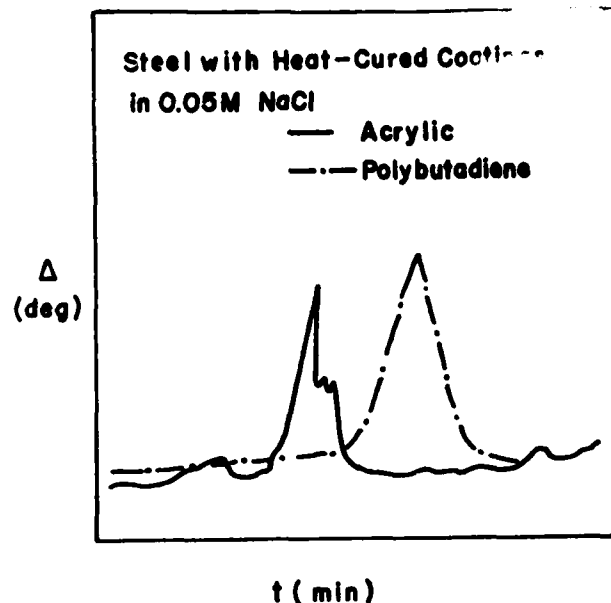


Fig. 1b - Same as Fig. 1a but the coatings were cured in air at 200°C

Distinguishing between Roughening and Film Growth or Dissolution

Fig. 2 shows Δ and ψ plots vs. time obtained using an automatic ellipsometer for an iron surface coated with a room temperature air-cured acrylic undergoing corrosion in 0.05M NaCl solution. Three regions can be delineated. The significance of these regions are described in Fig. 2. It can be seen in Fig. 2 that when $d\Delta/dt$ and $d\psi/dt$ have the same sign surface roughening or surface smoothing the coated iron is taking place; when $d\Delta/dt$ and $d\psi/dt$ have opposite signs, film growth or dissolution is occurring.

This interpretation of the behavior of Δ and ψ is based on our observations of uncoated iron in a buffered solution after carrying out potential cycling, a process which produces a smoother surface. More details are given in an earlier paper /2/.

Observing Corrosion Processes at Anodic and Cathodic Sites

Fig. 3a shows the arrangement developed by Ritter /3/ for studying the spatial development of subcoating cathodes and anodes using the ellipsometer. By puncturing one segment of the segmented specimen, one can promote the immediate formation of an anode on that specimen. This procedure then allows one to follow the real time development of cathodes on the unpunctured segment.

Fig. 3b gives the variation of Δ and pH (an important parameter in subcoating corrosion) with time for the anodic ("a") and cathodic ("c") segments. During the first 1400 min before the coating is punctured, there is little change in Δ for both segments. The pH varies between 5 and 8. When the segment "a" is punctured at 1400 min, thereby making it

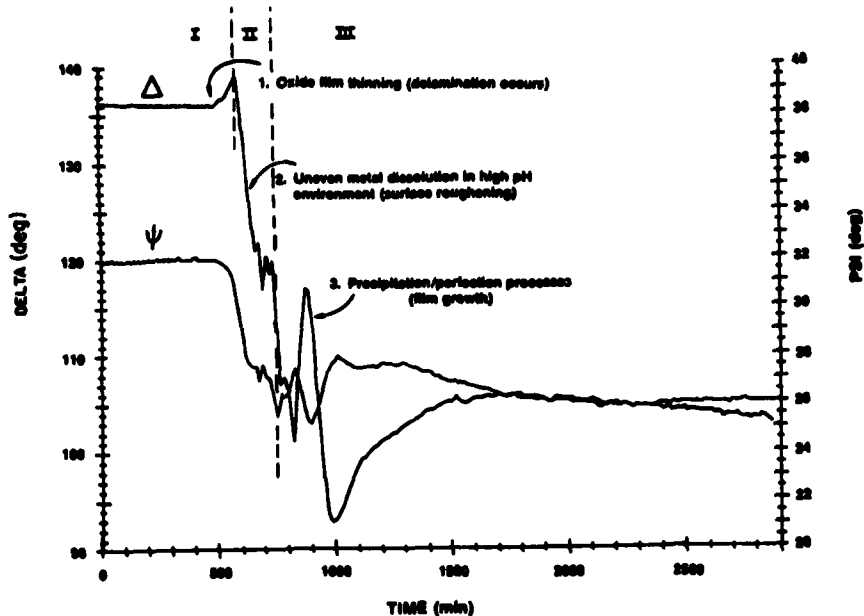


Fig. 2 - Δ and ψ plots vs. time made using an automatic ellipsometer for an iron/acrylic coating system undergoing corrosion in 0.05M NaCl solution.

the anode, a significant rise in Δ is observed. If the segments "a" and "c" are connected by joining the copper wire conductors attached to each (shown in Fig. 3a), the pH on "c" rises to about 13.5 and the Δ measured for "c" by the ellipsometer remains relatively constant. The change in Δ found for "a" however, is similar to that shown in Regions I and II in Fig. 2. When the conducting wires to "a" and "c" are disconnected, the subcoating pH drops to 8 in a few minutes. Reconnecting brings the pH back to 13 within 5 min. If the anodic and cathodic segments are left coupled for a few days, the subcoating pH on "c" declines, Δ for "a" decreases markedly while Δ for "c" also goes down but not as much.

A detailed discussion of the meaning of these results in terms of corrosion processes under coatings is given by Ritter in an earlier publication /3/.

Summary

1. It has been established that the ellipsometer is capable of revealing the effect of different organic coatings on the subcoating corrosion processes.

2. Using an automated ellipsometer, it has been demonstrated for the iron systems studied that when $d\Delta/dt$ and $d\psi/dt$ have opposite signs, corrosion product films are growing or dissolving and when they have the same sign, surface is becoming smoother or rougher.

Thus, surface roughening surface smoothing and film growth processes or dissolution can be identified.

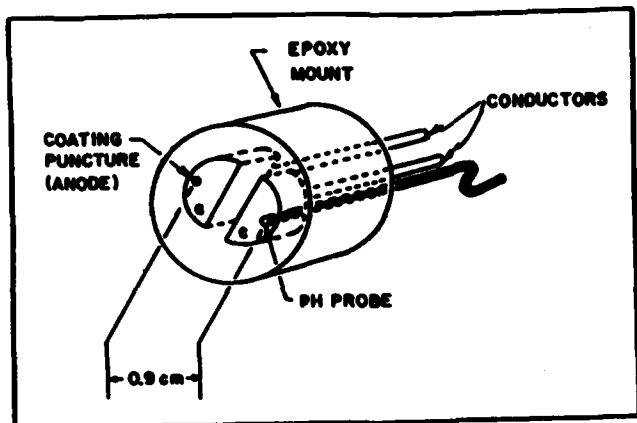


Fig. 3a - The segmented specimen that allows the ellipsometric examination of the development of anodic ("a") and cathodic ("c") sites on coated iron.

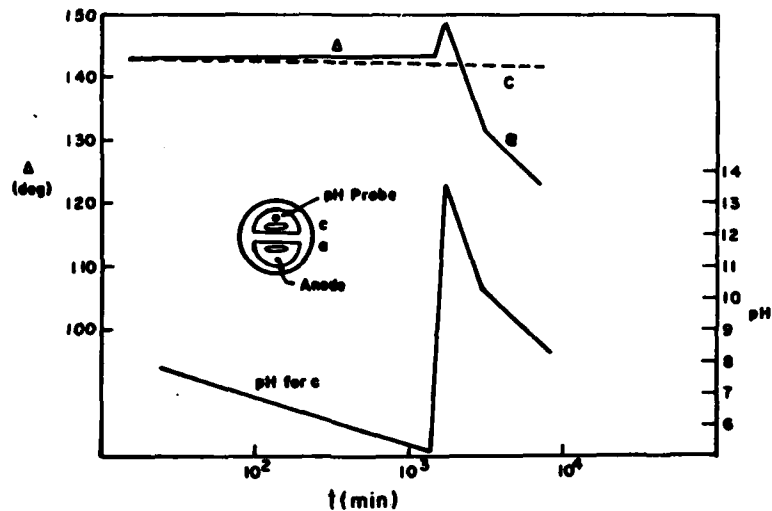


Fig. 3b - Δ , ψ and pH plotted vs time for a segmented iron/acrylic system in 0.05M NaCl solution. Inset shows the arrangement on the surface of the specimen, the ellipses shown being the regions studied ellipsometrically.

3. A segmented specimen has been developed that allows ellipsometric study of separate anodic and cathodic areas that form under an organic coating.

Acknowledgement

The authors are grateful to the Office of Naval Research who partially supported this work under contract No. NAONR 18-69. NRO 36-082

References

- /1/ RITTER, J.J. and KRUGER, J., Surf. Sci. 96 (1980) 364.
- /2/ RITTER, J.J. and KRUGER, J., Corrosion Control by Organic Coatings, H. Leidheiser, Jr., Ed., (National Association of Corrosion Engineers, Houston, TX) 1981, p. 28.
- /3/ RITTER, J.J., J. Coatings Technology 54 (1982) 51.

REPORT DOCUMENTATION PAGE		READ INSTRUCTIONS BEFORE COMPLETING FORM
1. REPORT NUMBER NBSIR 83-2790	2. GOVT ACCESSION NO. AD-A135	3. RECIPIENT'S CATALOG NUMBER 549
4. TITLE (and Subtitle) Passive Films Surface Structure and Stress Corrosion and Crevice Corrosion Susceptibility		5. TYPE OF REPORT & PERIOD COVERED Final Report 10/82 - 9/83
		6. PERFORMING ORG. REPORT NUMBER
7. AUTHOR(s) J. Kruger, J. J. Ritter, G. G. Long, M. Kuriyama and A. I. Goldman		8. CONTRACT OR GRANT NUMBER(s) NA ONR 18-69 NRO 36-082
9. PERFORMING ORGANIZATION NAME AND ADDRESS Inorganic Materials Div. and Metallurgy Div. National Bureau of Standards Washington, DC 20234		10. PROGRAM ELEMENT, PROJECT, TASK AREA & WORK UNIT NUMBERS 5610448
11. CONTROLLING OFFICE NAME AND ADDRESS Office of Naval Research Arlington, VA 22217		12. REPORT DATE Nov. 1983
		13. NUMBER OF PAGES
14. MONITORING AGENCY NAME & ADDRESS (if different from Controlling Office) Same as 11.		15. SECURITY CLASS. (of this report) Unclassified
		15a. DECLASSIFICATION/DOWNGRADING SCHEDULE
16. DISTRIBUTION STATEMENT (of this Report) Unlimited		
17. DISTRIBUTION STATEMENT (of the abstract entered in Block 20, if different from Report) Unlimited		
18. SUPPLEMENTARY NOTES		
19. KEY WORDS (Continue on reverse side if necessary and identify by block number) Passive films, organic coatings, chelating inhibitors, ellipsometry, EXAFS, iron oxide films, electrochemistry, cathodic delamination.		
20. ABSTRACT (Continue on reverse side if necessary and identify by block number) I. Iron K-absorption edge spectra were obtained from the passive films on iron for the dried films in air (<i>ex situ</i>) and for the films in the passi- vating solution (<i>in situ</i>). The <i>ex situ</i> results demonstrate that, while the structures of the films are more disordered than the spinel-like iron oxides (e.g. $\gamma\text{-Fe}_2\text{O}_3$), they are nevertheless closely related to these crystalline oxides. The <i>in situ</i> data shows evidence of a quite different structure, which may be due to the accommodation of hydrogen containing (Cont)		

Block 20 Cont'd

species into the structure.

II. Two sample-and-detector chambers for the study of surface films on metals using x-ray absorption spectroscopy are described. Results have been obtained using both a high intensity rotating anode x-ray generator and using the Cornell High Energy Synchrotron Source (CHESS).

III. The effects of chelating inhibitors on the cathodic delamination of an acrylic lacquer on iron have been studied by qualitative ellipsometry. The experiments indicate that both the chemical nature of the inhibitor and the mode of inhibitor introduction affect the rate of coating failure.

IV. The development of an ellipsometer technique to study corrosion under organic coatings has been advanced to 1) detect the effect of oxide film growth or dissolution, 2) distinguish between surface roughening and film growth, and 3) study corrosion on separate anodic and cathodic sites.

U.S. DEPT. OF COMM. BIBLIOGRAPHIC DATA SHEET (See instructions)	1. PUBLICATION OR REPORT NO. NBSIR 83-2790	2. Performing Organ. Report No.	3. Publication Date November 1983
4. TITLE AND SUBTITLE PASSIVE FILMS SURFACE STRUCTURE AND STRESS CORROSION AND CREVICE CORROSION SUSCEPTIBILITY			
5. AUTHOR(S) J. Kruger, J. J. Ritter, G. G. Long, M. Kuriyama, and A. I. Goldman			
6. PERFORMING ORGANIZATION (If joint or other than NBS, see instructions) NATIONAL BUREAU OF STANDARDS DEPARTMENT OF COMMERCE WASHINGTON, D.C. 20234		7. Contract/Grant No.	8. Type of Report & Period Covered
9. SPONSORING ORGANIZATION NAME AND COMPLETE ADDRESS (Street, City, State, ZIP) Inorganic Materials Div. and Metallurgy Div. National Bureau of Standards Washington, DC 20234			
10. SUPPLEMENTARY NOTES <input type="checkbox"/> Document describes a computer program; SF-185, FIPS Software Summary, is attached.			
11. ABSTRACT (A 200-word or less factual summary of most significant information. If document includes a significant bibliography or literature survey, mention it here) <p>I. Iron K-absorption edge spectra were obtained from the passive films on iron for the dried films in air (<u>ex situ</u>) and for the films in the passivating solution (<u>in situ</u>). The <u>ex situ</u> results demonstrate that, while the structures of the films are more disordered than the spinel-like iron oxides (e.g. $\gamma\text{-Fe}_2\text{O}_3$), they are nevertheless closely related to these crystalline oxides. The <u>in situ</u> data shows evidence of a quite different structure, which may be due to the accommodation of hydrogen containing species into the structure.</p> <p>II. Two sample-and-detector chambers for the study of surface films on metals using x-ray absorption spectroscopy are described. Results have been obtained using both a high intensity rotating anode x-ray generator and using the Cornell High Energy Synchrotron Source (CHESS).</p> <p>III. The effects of chelating inhibitors on the cathodic delamination of an acrylic lacquer on iron have been studied by qualitative ellipsometry. The experiments indicate that both the chemical nature of the inhibitor and the mode of inhibitor introduction affect the rate of coating failure.</p> <p>IV. Ellipsometric study of corrosion under paints advanced to 1) detect film dissolution, 2) separate surface roughening and film growth effects, 3) study anodes & cathode</p>			
12. KEY WORDS (Six to twelve entries; alphabetical order; capitalize only proper names; and separate key words by semicolons) cathodic delamination; chelating inhibitors; electrochemistry; electrochemistry; ellipsometry; EXAFS; iron oxide films; organic coatings; passive films			
13. AVAILABILITY <input checked="" type="checkbox"/> Unlimited <input type="checkbox"/> For Official Distribution. Do Not Release to NTIS <input type="checkbox"/> Order From Superintendent of Documents, U.S. Government Printing Office, Washington, D.C. 20402. <input checked="" type="checkbox"/> Order From National Technical Information Service (NTIS), Springfield, VA. 22161		14. NO. OF PRINTED PAGES 46	15. Price \$8.50

END

FILMED

1-84

DTIC